Heliyon 10 (2024) e40630

Contents lists available at ScienceDirect

Heliyon

journal homepage: www.cell.com/heliyon

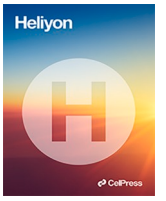

Research article

Synthesis and pharmacological evaluation of heteroarylamide derivatives as potential analgesic, anti-inflammatory, antidiarrheal and cytotoxic agents

Nazifa Tabassum [a], Sabiha Enam Spriha [a], Poushali Saha [a], Fahad Imtiaz Rahman [a], A.S.M. Monjur Al Hossain [b], S. M. Abdur Rahman [a,c,*]

[a] Department of Clinical Pharmacy and Pharmacology, University of Dhaka, Dhaka, 1000, Bangladesh
[b] Department of Pharmaceutical Technology, University of Dhaka, Dhaka, 1000, Bangladesh
[c] Biomedical Research Center, University of Dhaka, Dhaka, 1000, Bangladesh

ARTICLE INFO

Keywords:
Antidiarrheal
Cytotoxic
Heteroarylamides
Synthesis
Peripheral analgesic

ABSTRACT

Six heteroarylamide derivatives were synthesized in good yields and screened for several biological activities. Compounds **1–5** demonstrated analgesic activity with percentage inhibition of writhing between 77.10 and 95.79 %, comparable to that of the standard aceclofenac having 91.12 % writhing inhibition. Evaluation of anti-inflammatory activity unveiled that compound **4** exhibited 36.9 %, 64.17 %, 82.9 % and 93.9 % inhibition of paw edema as compared to aceclofenac's inhibition of 35.5 %, 78.6 %, 79.3 % and 91.2 % at the 1st, 2nd, 3rd and 4th hours, respectively. Compounds **5** and **6** exerted considerable antidiarrheal effects with 85.00 % and 71.67 % inhibition of defecation at 25 mg/kg dose, respectively, whereas, the standard loperamide showed 85.00 % inhibition. Compounds **4–6** manifested promising activity in brine shrimp lethality bioassay as well as in trypan blue dye exclusion assay, resulting in 10–20 % cell viability on HeLa cell line and compound **5** was found to have the lowest IC_{50} of 281.96 μM in the MTT assay. Molecular docking analysis suggested that certain macromolecular targets such as cyclooxygenase-2, muscarinic M3 receptor and matrix metalloproteinase 9 (MMP9) might be involved for the observed activities. As predicted by *in silico* ADME/T analysis, the compounds also possessed good pharmacokinetic properties.

1. Introduction

Carboxamides are well known functional entities that have been identified as important part of several existing medications (Fig. 1a–f) and, thus, are interesting targets for new drug development. Several carboxamides are currently in use for mitigation of diversified range of disorders. Nitazoxanide, a carboxamide derivative (Fig. 1**a**), is an FDA-approved antiprotozoal and antibacterial drug [1] which is also reported to possess anticancer and antiviral activity [2,3]. Ahmed and co-workers recently reported the antibacterial, anti-inflammatory and cytotoxic effects of heteroaryl derivatives of nitazoxanide [4,5]. Loperamide (Fig. 1**b**) which serves as a long acting antidiarrheal agent also contains amide linkages [6]. Several tyrosine kinase inhibitors such as dasatinib, nilotinib (Fig. 1**c** and **d**), and imatinib which are principally used in chronic myeloid leukemia (CML) treatment possess carboxamide functional

* Corresponding author. Department of Clinical Pharmacy and Pharmacology, University of Dhaka, Dhaka, 1000, Bangladesh.
E-mail address: smarahman@du.ac.bd (S.M.A. Rahman).

https://doi.org/10.1016/j.heliyon.2024.e40630
Received 15 June 2024; Received in revised form 23 October 2024; Accepted 20 November 2024
Available online 22 November 2024

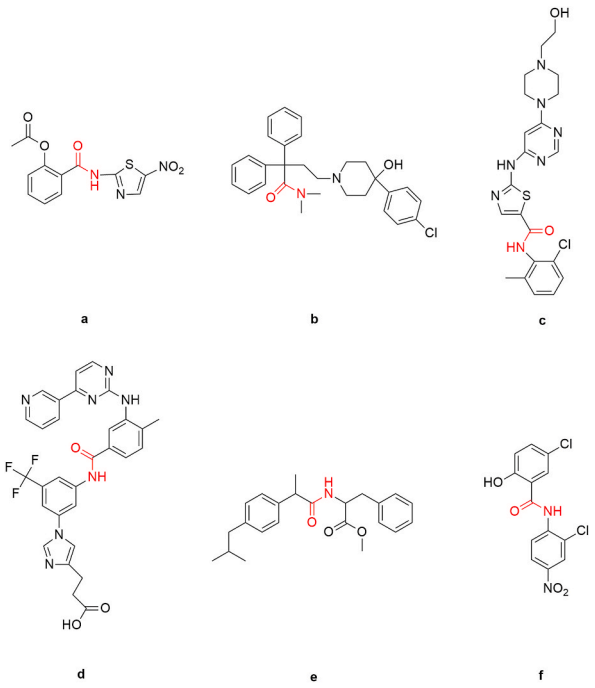

Fig. 1. Structure of medicinally important drugs containing aryl amide group; a) nitazoxanide, b) loperamide, c) dasatinib, d) nilotinib, e) amide prodrug of ibuprofen and f) niclosamide.

groups.

Pain, which can be considered as a part of body's protective mechanism, is perceived as a sensation due to tissue damage and can occur with or without inflammation. Often being associated with pain, inflammation is multifactorial and a wide range of features are characteristic of inflammation including redness, swelling, tissue function loss, and heat [7,8]. Cyclooxygenase enzymes (COX) are associated with inflammatory and pain responses as these enzymes are involved in the formation of prostanoids. As a result, COX inhibitors are popularly used for the treatment of pain and inflammatory conditions. Although NSAIDs' are the most popular group of COX inhibitors, numerous side effects like stomach ulcer, cardiovascular events and renal disturbances are associated with them [9,10]. Several analgesic and anti-inflammatory drugs when developed as their amide derivatives were found to possess better pharmacokinetic and pharmacodynamic properties. The amide prodrug of naproxen and ibuprofen (Fig. 1**e**), for instance, showed better activity than their parent drugs [11]. Some amide derivatives of indomethacin exhibited selectivity against the COX-2 enzyme and, thus, are capable of reducing the side effects associated with the non-selectivity of the parent molecule [12].

Among the carboxamides, diarylamides are promising structural analogs possessing potential biological activities. Several diarylamides are found to possess promising anticancer activity [13]. Niclosamide (Fig. 1**f**) is another diarylamide derivative that has been used as an anthelmintic drug and is now being indicated in several disorders including cancer, infectious diseases, metabolic disorders, and others [14]. Thus, considering the prospect of the diarylamide moiety and the ease of their synthetic procedure we synthesized six heteroarylamide derivatives for which different *in vivo* and *in vitro* pharmacological screening were accomplished.

In silico studies are computational methods widely applied for understanding potential mechanism underlying the given effects by any substance. Finding of lead compounds and designing of drugs based on chemical structures are markedly dependent on *in silico* approaches [15]. Previously many studies exploited the advantages of computational studies to verify their findings as well as for potential mechanism of action and lead finding [16,17]. Thus, we aimed at *in silico* analysis to investigate the presumed molecular mechanism accountable for the effects given by the synthesized molecules.

2. Materials and methods

2.1. General experimental procedure

The glassware and apparatus utilized in the synthesis procedure were well dried before use. The solvents (ethyl acetate, n-hexane, dichloromethane, chloroform) were subjected to distillation prior to use. To track the progression of all reactions, thin layer chromatography (TLC), coupled with the requisite spot detection on TLC plates (Sigma-Aldrich) using UV light at 254 nm was utilized. Silica gel 60 (0.06–0.2 mm, ROTH) was used in column chromatography for purification. ^{1}H NMR (400 MHz) spectroscopic analysis of the synthesized compounds was done by Bruker 400 NMR instrument using $CDCl_3$ solvent. ^{13}C NMR was done by using Bruker 150 NMR instrument; $CDCl_3$ and CD_3OD was used as solvent. Shimadzu IRSpirit was used to record Fourier-transform (FT-IR) spectra.

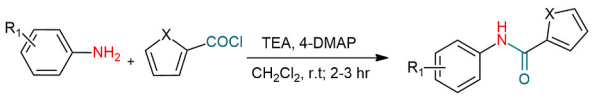

Fig. 2. Scheme 1: Synthetic scheme for heteroarylamide derivatives.

Table 1
Synthesis of various heteroaryalamide derivatives.

Entry no	R_1	X	Product (Yield %)
1	*p*-NO_2	X=S	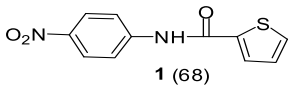 **1** (68)
2	*p*-NO_2	X=O	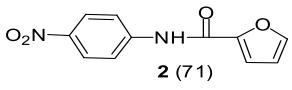 **2** (71)
3	*o*-NO_2 *p*-Cl	X=S	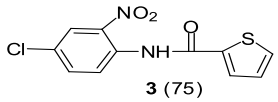 **3** (75)
4	*o*-NO_2 *p*-Cl	X=O	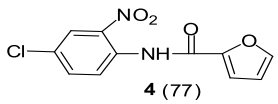 **4** (77)
5	*m*-NO_2	X=S	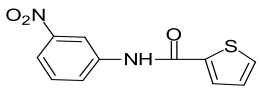 **5** (85)
6	*m*-NO_2	X=O	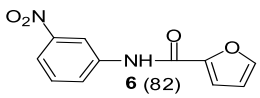 **6** (82)

Reagents and solvents were purchased from Sigma Aldrich, Germany.

2.2. General synthetic procedure of the heteroarylamide derivatives

Calculated amount (200 mg/1 equivalent) of starting materials (various aniline derivatives) in dichloromethane along with the catalysts triethyl amine (TEA) and 4-(dimethyl amino)-pyridine (DMAP) were stirred at 5 °C for 15 min. Rest of the reaction was carried out at room temperature. 2–3 equivalents of acid chlorides were then added to that mixture with continuous stirring. Upon completion of the reaction, the mixture was quenched by addition of 0.1N sodium hydroxide (NaOH). The resultant mixture was subjected to extraction by using dichloromethane followed by washing with brine solution. The extract was dried using anhydrous sodium sulphate. Finally, using a rotatory evaporator, solvent was removed and further purification of the test compounds was performed by using column chromatography. The reaction scheme and products are shown in Fig. 2 and Table 1, respectively.

2.3. Spectroscopic characterization of synthesized heteroarylamide derivatives

^{1}H NMR, ^{13}C NMR and FTIR were employed to characterize the compounds. Data obtained were compared to previously reported data for confirmation.

2.3.1. *N-(4-nitrophenyl)thiophene-2-carboxamide (1)*

4-nitroaniline, the starting material, and 2-thiophenecarbonyl chloride reacted in dichloromethane solvent at room temperature. IR (cm^{-1}): 3362, 3104, 2917, 2848, 1642, 1538; ^{1}H NMR (400 MHz, TMS, $CDCl_3$, δ/ppm): δ 7.17 (t, J = 4 Hz, 1 H), δ 7.62 (dd, J =

4.8Hz, 1.2 Hz, 1H), δ 7.68 (dd, J = 3.6 Hz, 0.8 Hz, 1H), δ 7.81 (m, 2H), δ 7.92 (s, 1H), δ 8.26 (m, 2H). ^{13}C NMR (150 MHz, $CDCl_3$, δ/ppm): 160, 144, 143, 139, 132, 129, 128, 125 (2C), 119 (2C).

2.3.2. N-(4-nitrophenyl)furan-2-carboxamide (2)

4-nitroaniline and 2-furancarbonyl chloride reacted under room temperature leading to the formation of *N*-(4-nitrophenyl)furan-2-carboxamide (**2**).

IR (cm^{-1}): 3341, 3127, 2921, 2849, 1663, 1545; ^{1}H NMR (400 MHz, TMS, $CDCl_3$, δ/ppm): δ 6.61 (dd, J = 3.6 Hz, 2 Hz, 1H), δ 7.32 (dd, J = 3.4 Hz, 0.8 Hz, 1H), δ 7.56 (dd, J = 2Hz, 0.8 Hz, 1H), δ 7.84 (m, 2H), δ 8.26 (m, 2H), δ 8.32 (s, 1 H). ^{13}C NMR (150 MHz, $CDCl_3$, δ/ppm): 156, 147, 144, 143.85, 143.27, 125 (2C), 119 (2C), 116, 113.

2.3.3. N-(4-chloro-2-nitrophenyl)thiophene-2-carboxamide (3)

4-chloro-2-nitroaniline which upon reaction with 2-thiophenecarbonyl chloride at room temperature using dichloromethane as solvent resulted in formation of compound **3.**

IR (cm^{-1}); 3329, 31254, 3094, 1679, 1579; ^{1}H NMR (400 MHz, TMS, $CDCl_3$, δ/ppm): δ 7.19 (t, J = 4 Hz, 1H), δ 7.65 (m, 2H), δ 7.745 (dd, J = 4Hz, 1.2 Hz, 1H), δ 8.27 (d, J = 2.8 Hz, 1H), δ 8.93 (d, J = 9.2 Hz, 1H), δ 11.21 (s, 1H). ^{13}C NMR (150 MHz, $CDCl_3$, δ/ppm): 160, 138, 136.26, 136.21, 133, 132, 129, 128.46, 128.27, 125, 123.

2.3.4. N-(4-chloro-2-nitrophenyl)furan-2-carboxamide (4)

Condensation reaction between 4-chloro-2-nitroaniline and 2-furancarbonyl chloride at room temperature using DMAP and TEA as catalyst led to the formation of *N*-(4-chloro-2-nitrophenyl)furan-2-carboxamide (**4**).

IR (cm^{-1}): 3333, 3130, 3085, 1679, 1585; ^{1}H NMR (400 MHz, TMS, $CDCl_3$, δ/ppm): δ 6.60 (dd, J = 3.2 Hz, 1.6 Hz, 1H), δ 7.32 (dd, J = 3.6, 0.8 Hz, 1H), δ 7.64 (m, 2H), δ 8.26 (d, J = 2.8 Hz, 1H), δ 8.95 (d, J = 9.2 Hz, 1H), δ 11.36 (s,1H). ^{13}C NMR (150 MHz, $CDCl_3$, δ/ppm): 158, 147, 145, 136.51, 135.99, 133, 128, 125, 125, 116, 112.

2.3.5. N-(3-nitrophenyl)thiophene-2-carboxamide (5)

3-nitroaniline and 2-thiphenecarbonyl chloride upon reaction under room temperature using TEA and DMAP as catalyst resulted in the formation of *N*-(3-nitrophenyl)thiophene-2-carboxamide (**5**).

IR (cm^{-1}): 3380, 3088, 1655, 1595; ^{1}H NMR (400 MHz, TMS, $CDCl_3$, δ/ppm): δ 7.16 (t, J = 4 Hz, 1H), δ 7.54 (t, J = 8.4 Hz, 1H), δ 7.61 (d, J = 4.8 Hz, 1H), δ 7.69 (d, J = 3.2 Hz, 1H), δ 7.93 (s, 1H), δ 7.99 (d, J = 8.4 Hz, 1H), δ 8.07 (d, J = 8.4 Hz, 1H), δ 8.45 (s, 1H). ^{13}C NMR (150 MHz, $CDCl_3$, δ/ppm): 160, 148, 139, 138, 131, 129, 127, 126, 123, 118, 114.

2.3.6. N-(3-nitrophenyl)furan-2-carboxamide (6)

N-(3-nitrophenyl)furan-2-carboxamide (**6**) was formed using 3-nitroaniline and 2-furancarbonyl chloride as starting material.

IR (cm^{-1}): 3306, 3140, 3084, 1658, 1563; ^{1}H NMR (400 MHz, TMS, $CDCl_3$, δ/ppm): δ 6.59 (dd, J = 3.6Hz, 1.6Hz, 1H), δ 7. 30 (dd, J = 3.6 Hz, 0.8 Hz, 1H), δ 7.53 (m, 2H), δ 7.99 (m, 1H), δ 8.08 (m, 1H), δ 8.26 (s, 1H), δ 8.49 (t, J = 2.4 Hz, 1H). ^{13}C NMR (150 MHz, $CDCl_3$, δ/ppm): 156, 148, 146, 144, 138, 129, 125, 118, 116, 114, 112.

2.4. Evaluation of analgesic activity

Evaluation of the analgesic activity was carried out by counting the numbers of squirms in mice treated with acetic acid and test samples [18]. Aceclofenac, as standard, and the test samples were given orally to the experimental animals at two different doses, i.e. low dose (25 mg/kg) and high dose (50 mg/kg) [19,20]. After 30 min, 0.7 % acetic acid was injected intraperitoneally to each of the animals of every group. The number of squirms in each mouse was counted after 5 min of acetic acid injection for 15 min. Comparisons were drawn among the average writhing count of test groups to that of the control.

2.5. Evaluation of anti-inflammatory activity

Carrageenan induced paw edema method was used for anti-inflammatory activity evaluation [21,22]. Eight groups (standard, control, and the six test sample groups) consisting of 5 rats in each group received predetermined treatment by oral route. Aceclofenac as the standard and the test samples were given at 100 mg/kg dose. The right hind paw volume of test animals was measured at 0^{th} hour using a plethysometer (before the injection of carrageenan) which was the baseline reading. Paw volumes were recorded again at 1st, 2nd, 3rd and 4th hour followed by carrageenan injection. The mean increase in the volume of injected hind paw was calculated.

2.6. Cytotoxicity assay

The cytotoxic potential of the test samples was screened by brine shrimp lethality bioassay, trypan blue exclusion assay and MTT assay on HeLa cell line. HeLa cell line was procured from the Graduate School of Medicine, Gunma University, Gunma, Japan. The cell line was exclusively maintained in DMEM (Dulbecco's Modified Eagles Medium) which contains 1 % penicillin-streptomycin (1:1), 0.2 % gentamycin and 10 % fetal bovine serum (FBS).

Table 2
Evaluation of analgesic activity.

Sample Code	Dose (mg/kg)	Number of Writhing (Mean ± SEM)	% Inhibition of writhing
Control	0.1 ml/10 gm	21.4 ± 0.68	100
Standard (Aceclofenac)	25	1.9 ± 0.332***	91.12
1	25	4.5 ± 0.500 ***	78.97
	50	1.4 ± 0.187***	93.46
2	25	4.9 ± 0.332***	77.10
	50	2.2 ± 0.370***	89.72
3	25	1.4 ± 0.240***	93.46
	50	3. 2 ± 0.370***	85.05
4	25	1.4 ± 0.187***	93.46
	50	0.9 ± 0.245***	95.79
5	25	1.4 ± 0.240***	93.46
	50	2.6 ± 0.240***	87.85
6	25	12.4 ± 0.510***	42.06
	50	15.2 ± 0.730**	28.97

Note: ***p < 0.001, **p < 0.01 compared to control.

Table 3
Evaluation of mean paw volume.

Sample code	Mean Paw Volume in ml (Percentage inhibition)				
	0^{th} hour	1st hour	2nd hour	3rd hour	4th hour
Control	0.412 ± 0.0191	0.688 ± 0.0269	0.786 ± 0.0121	0.788 ± 0.0153	0.774 ± 0.022
Standard (Aceclofenac)	0.516 ± 0.0108**	0.694 ± 0.0172 (35.5)	0.596 ± 0.014*** (78.6)	0.564 ± 0.0129*** (79.3)	0.548 ± 0.0215*** (91.2)
1	0.554 ± 0.0439*	0.838 ± 0.0159** (18.8)	0.928 ± 0.0116*** (16)	0.712 ± 0.0258* (73.9)	0.66 ± 0.0224** (87.3)
2	0.622 ± 0.0242***	0.896 ± 0.0232*** (0.725)	0.894 ± 0.0136*** (27.2)	0.598 ± 0.0252*** (93.6)	0.522 ± 0.0120 (72.4)
3	0.63 ± 0.0161***	0.720 ± 0.0184* (67.4)	0.89 ± 0.017** (30.5)	0.688 ± 0.0128* (84.6)	0.692 ± 0.0128* (82.9)
4	0.562 ± 0.0136	0.736 ± 0.0133* (36.9)	0.696 ± 0.0068*** (64.17)	0.626 ± 0.0169*** (82.9)	0.584 ± 0.0117*** (93.9)
5	0.588 ± 0.0086***	0.86 ± 0.0141*** (1.45)	0.854 ± 0.0121** (28.9)	0.794 ± 0.012* (45.2)	0.724 ± 0.0154* (62.4)
6	0.628 ± 0.0128***	0.9 ± 0.0107*** (21.7)	0.928 ± 0.0156*** (19.8)	0.9 ± 0.0114*** (42.6)	0.856 ± 0.0125* (37.01)

Note: ***p < 0.001, **p < 0.001, *p < 0.05 compared to control.

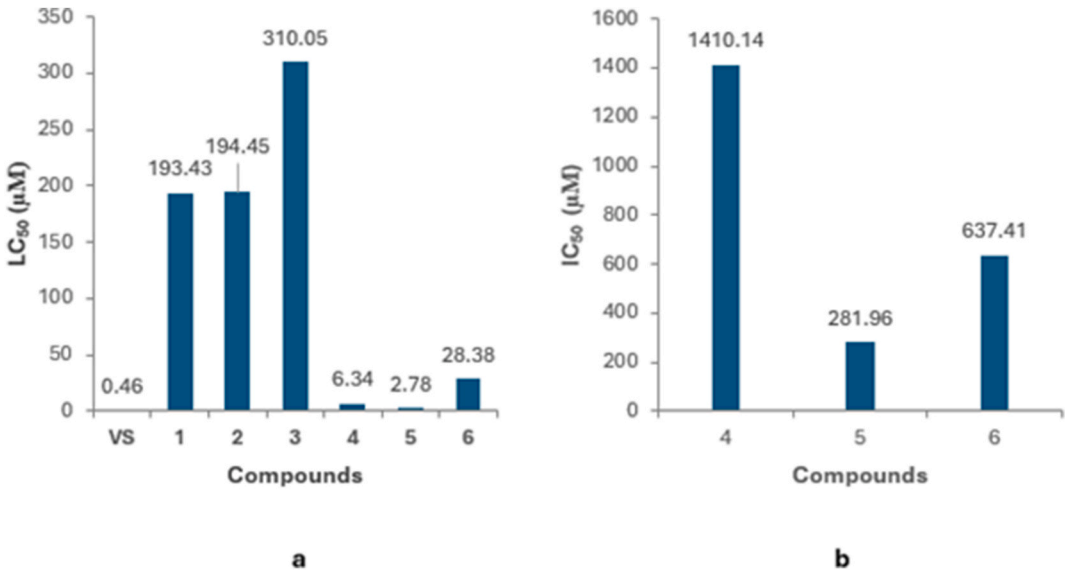

Fig. 3. Cytotoxic effect of heteroarylamide derivatives measured by **a)** brine shrimp lethality bioassay (cytotoxicity measured by LC_{50}). **b)** MTT assay (cytotoxicity measured by IC_{50}).

Table 4
Survivability of HeLa cells upon treatment with synthesized samples.

Compound	Concentration (μg/ml)	Survival of cells
Negative control	–	100 %
Positive control	–	>95 %
1	500	>95 %
2	500	>95 %
3	500	>95 %
4	500	10–20 %
5	500	10–20 %
6	500	10–20 %

Table 5
Anti-diarrheal activity of synthesized compounds.

Compound	Dose (mg/kg)	Mean number of defecated pellets of 5 mice in 4 h ±SEM	% Inhibition of defecation comparing against control
Control	0.1 ml/10 gm	12 ± 0.55	–
Standard (Loperamide)	25	1.8 ± 0.37***	85.00
1	25	10.8 ± 0.49	10.00
	50	8.6 ± 1.21*	28.33
2	25	6.6 ± 1.40**	45.00
	50	7.8 ± 1.16*	35.00
3	25	3 ± 0.45 ***	75.00
	50	6.8 ± 086***	43.33
4	25	6.2 ± 0.49***	48.33
	50	2.6 ± 0.24***	78.33
5	25	1.8 ± 0.37***	85.00
	50	1.6 ± 0.4***	86.67
6	25	3. 4 ± 0.68***	71.67
	50	2.00 ± 0.32***	83.33

Note: ***$p < 0.001$, **$p < 0.01$, *$p < 0.1$ compared with control.

Table 6
Binding affinity and binding interaction of the synthesized compounds with COX-2 (PDB ID: 5IKT).

Ligand	Binding Affinity (kcal/mol)	H-bond (Å)	Hydrophobic Interactions and other Interactions
Aceclofenac	−7.4	Tyr348A (2.65) Ser530A (2.23)	Tyr385A, Ser530A, Leu352A, Val523A, Ala527A, Leu531A, Arg120A, Val349A, Ser530A
1	−7.5	–	Ala527A, Val349A, Leu352A, Trp387A, Met522A, Phe381A
2	−7.8	Ser530A (2.59), Arg120A (2.68)	Leu352A, Leu359A, Ala527A, Val349A, Leu531A
3	−7.2	Tyr385A (1.80)	His207A, His388A, Gln203A, Leu391A, Leu390A, Ala199A
4	−6.4	Thr212A (2.41), Asn382A (2.85)	His386A, Lys211A, Leu294A, His207A, Val291A,
5	−7.6	His388A (2.66), Asn382A (2.39), Thr212A (2.91)	His386A, Ala202A, His207A, His388A
6	−7.8	His207A (2.74)	Gln203A, Ala202A, His207A

2.6.1. Brine shrimp lethality bioassay

This test acts as an initial indicator of potential cytotoxic effects of sample compounds. Brine shrimp nauplii were treated with divergent concentrations of the test samples and cell survival was counted afterward. Finally, the logarithmic values of the sample concentration were plotted against the shrimp death percentage to determine the median lethal concentration (LC_{50}) [23]. From the curve data, the best-fitted line was then determined by regression analysis.

2.6.2. Assessment of cytotoxic activity on HeLa cell line

2.6.2.1. Trypan blue dye exclusion test. Human cervical carcinoma cell line also known as HeLa, is popularly used in determination of the cytotoxicity of any test compound. The test is a means of qualitative evaluation of cytotoxicity [24]. In this method, the cell line was treated with DMEM or Dulbecco's Modified Eagles' Medium for their maintenance and test samples were added to the cell line after incubation. 1 part of diluted cell suspension was then treated with 1 part of 0.4 % trypan blue and for 3 min incubation was done [25]. An inverted microscope was used for visualization of cytotoxicity.

2.6.2.2. MTT assay. The compounds which gave positive results in qualitative analysis of cytotoxicity was subjected to quantitative analysis. To calculate the IC_{50} of the test compounds, the MTT (3-(4,5-dimethylthiazol-2-yl)-2,5-diphenyl-2H-tetrazolium bromide)

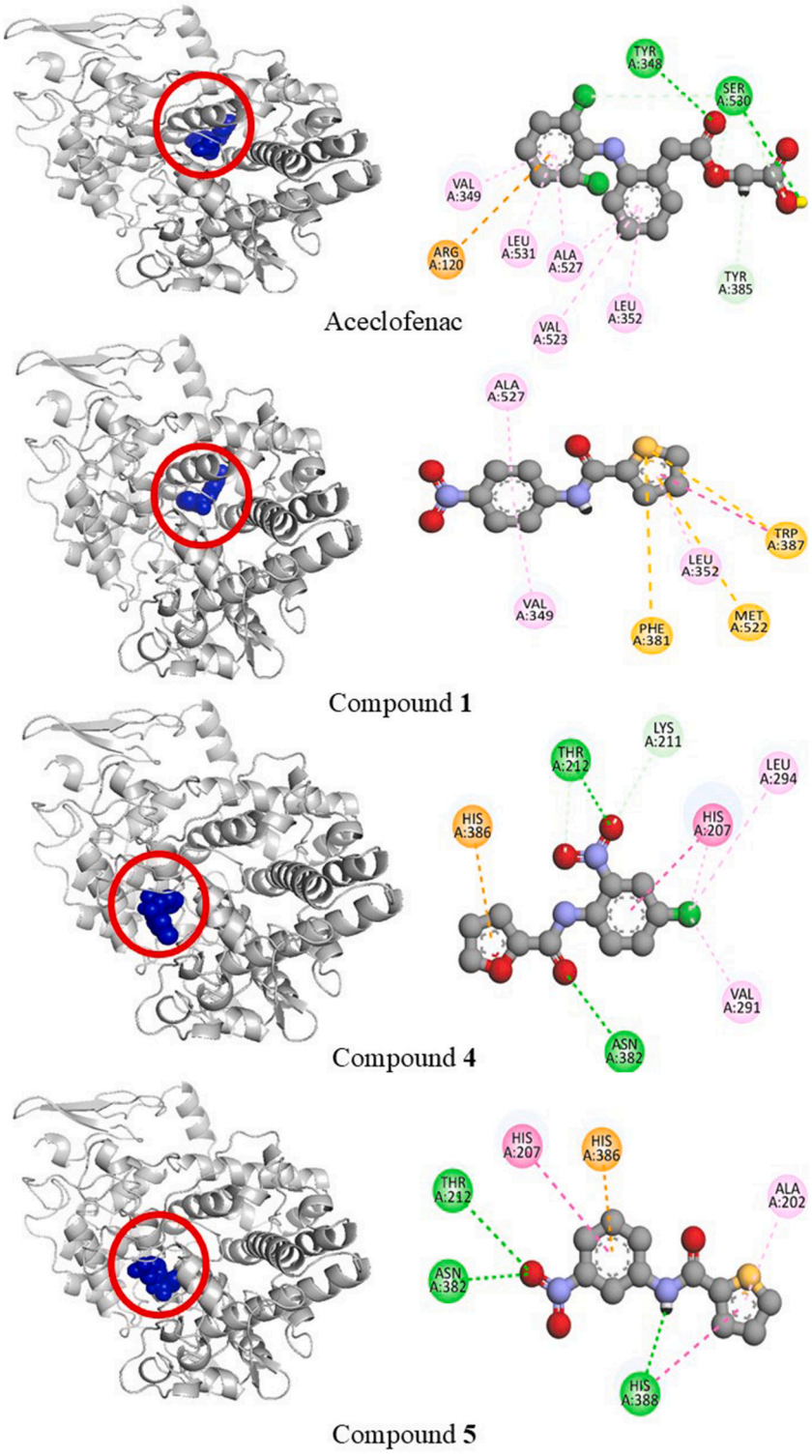

Fig. 4. Interaction between cyclooxygenase-2 with aceclofenac, compounds **1**, **4**, and **5.** Green: conventional hydrogen bond, pink-violet: hydrophobic, orange: pi-cation/pi-anion/pi-sulfur, cyan: carbon-hydrogen bond. (For interpretation of the references to colour in this figure legend, the reader is referred to the Web version of this article.)

Table 7
Binding affinity and binding interaction with kappa opioid receptor (PDB ID: 6VI4).

Ligand	Binding Affinity (kcal/mol)	H-bond (Å)	Hydrophobic Interactions and other Interactions
Loperamide	−9.2	–	Leu184A, Ile191A, Val195A, Ser136B, tyr140B, Ile180B, Trp183B
1	−6.6	Leu184A (2.06)	Ile191A, Ser 88A, Leu184A
2	−6.9	–	Ile91A, Ser188A, Ser187A, Ile180B, Trp183B, Ser187B
3	−7.6	–	Ile191A, Ser192A, Val195A, Phe99B, Ile180B, Trp183B
4	−7.5	–	Ile191A, Ser192A, Val5A, Lys176B, Ile180B, Trp183B
5	−7.2		Ser188A, Ile191A, Val195A, Trp183B
6	−7.3	–	Leu184A, Ile191A, Ile180B, Trp183B

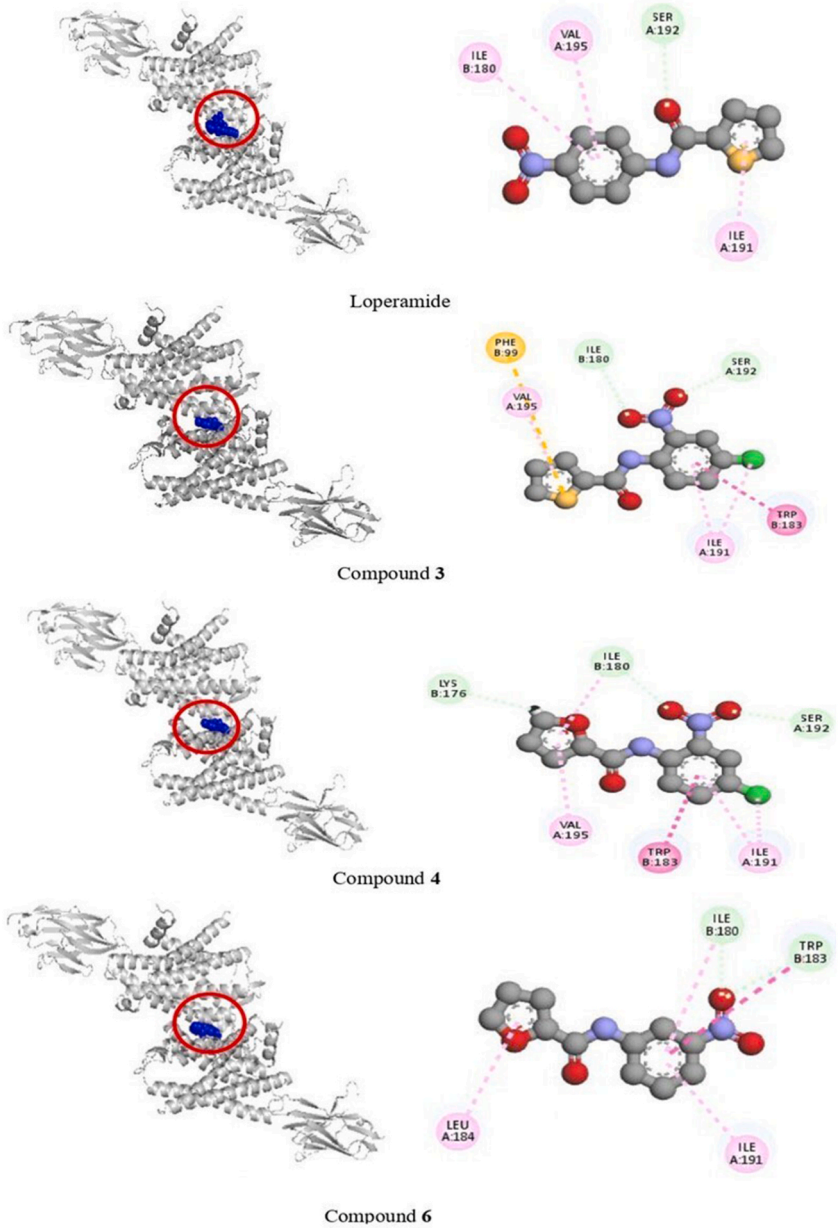

Fig. 5. Interaction between kappa opioid receptor with loperamide, compounds **3**, **4**, and **6.** Green: conventional hydrogen bond, pink-violet: hydrophobic, orange: pi-cation/pi-anion/pi-sulfur, cyan: carbon-hydrogen bond. (For interpretation of the references to colour in this figure legend, the reader is referred to the Web version of this article.)

Table 8
Binding affinity and binding interaction with M3 muscarinic receptor (PDB ID: 4DAJ).

Ligand	Binding Affinity (kcal/mol)	H-bond (Å)	Hydrophobic Interactions and other Interactions
Darifenacin	−7.7	–	Leu497B, Ile500B, Ile501B, Trp251B, Thr504B, Pro505B
1	−7.3	–	Tyr529B, Trp503B, Ser151B, Cys532B, Tyr 148B, Ala235B, Val510B
2	−7.5	–	Tyr529B, Trp503B, Thr213B Cys532B, Tyr148B, Ala 235B, Val510B
3	−8.1	Asn507B (2.64)	Tyr148B, Ala235B, Trp503B, Cys532B, Tyr533B
4	−8.1	–	Ser151B, Ala235B, Trp510B, Val510B, Tyr529B, Cys532B
5	−8.0	–	Ser151B, Ala235B, Ala238B, Trp503B, Tyr506B, Tyr529B, Cys532B
6	−8.0	–	Ser151B, Ala235B, Ala238B, Trp503B, Tyr506B, Tyr529B, Cys532B

assay was performed. It is a technique used for the quantitative evaluation of cytotoxicity expressed as half maximal inhibitory concentration (IC_{50}) [26]. Here the cell culture was treated with MTT substrate and incubated for 1–4 h. The process was then followed by solubilizing the test cells and formazan products in DMSO and measurement of absorbance at 570 nm [27].

2.7. Evaluation of antidiarrheal activity

Antidiarrheal potential of the test samples was evaluated using the method of castor oil induced diarrhea [28]. Standard loperamide was given at a dose of 25 mg/kg. The synthesized test samples were given at 25 mg/kg and 50 mg/kg doses. Upon treating mice with 0.5 ml castor oil orally, an observation period of 4 h was given. The fecal consistency and the frequency of defecation were recorded.

2.8. Evaluation of antioxidant activity

2,2-Diphenyl-1picrylhydrazyl (DPPH) assay was employed for the evaluation of the antioxidant activity of the synthesized samples [29]. Methanolic solution of the test samples at different concentrations were taken and to it DPPH (concentration 101.44 μM) was incorporated. Upon completion of an incubation period at 37 °C for 30 min, measurement of absorbance was done at 517 nm wavelength. Later, sample concentrations were plotted against the percentage inhibition from which the IC_{50} was calculated.

2.9. Molecular docking study

For molecular docking, crystallographic structures of the target proteins i.e. cyclooxygenase-2 (COX-2) (PDB ID: 5IKT), kappa opioid receptor (PDB ID: 6VI4), muscarinic M3 receptor (PDB ID: 4DAJ), β tubulin (PDB ID:1SA0), human topoisomerase-II (PDB ID:3QX3), matrix metalloproteinase 9 (MMP9) (PDB ID: 4XCT), Src homology (PDB ID: 2H8H) and peroxisome proliferator-activated receptor gamma/PPAR-γ (PDB ID: 4HEE) were retrieved from RCSB Protein Data Bank (RCSB-PDB) in PDB format [30]. ChemDraw Ultra (version 12.0.2) was used for drawing ligands. Receptor-ligand interactions were studied at corresponding active sites of target proteins using AutoDock Vina. The coordinates of the grid box (X, Y, Z) for COX-2 (PDB ID: 5IKT), kappa opioid receptor (PDB ID: 6VI4), muscarinic M3 receptor (PDB ID: 4DAJ), β tubulin (PDB ID: 1SA0), human topoisomerase II (PDB ID: 3QX3), MMP9 (PDB ID: 4XCT), Src homology (PDB ID: 2H8H) and PPAR-γ (PDB ID: 4HEE) were (158.98, 200.37, 209.54), (54.94, −51.57, −17.38), (−35.94, 10.66, −40.41), (30.05, 11.04, 49.98), (28.30, 102.87, 68.05), (−17.69, −10.42, 17.13), (19.89, −8.99, 14.40) and (19.48, 32.90, 66.72) respectively. Biovia Discovery Studio Client 2021 was utilized for the visualization of interactions.

2.10. ADME/T prediction

Five specific parameters i.e. molecular weight, lipophilicity, hydrogen bond donors' number and number of acceptors of hydrogen bond (H-bond), molar refractivity which are collectively known as Lipinski's rule of five for drug-likeness were predicted by SwissADME [31]. Absorption, distribution, metabolism, excretion (ADME) and toxicological properties were predicted for the synthesized samples using online server admetSAR (http://lmmd.ecust.edu.cn/admetsar2/).

2.11. Statistical analysis

One way analysis of variance (ANOVA) was used for the evaluation of statistical significance of the obtained results. The values were expressed in terms of mean ± SEM (n = 5). The data for which p value was obtained as $p < 0.05$ were considered significant. Microsoft excel (version 2011) and GraphPad prism (version 10.2.2) were used for analysis of the acquired data.

3. Results

3.1. Synthesis of heteroarylamide derivatives

The synthetic procedure utilized several aniline derivatives as starting material which upon reaction with different types of heteroaryl acid chlorides resulted in a variety of heteroarylamide derivatives. TEA and 4-DMAP were used as base and catalyst

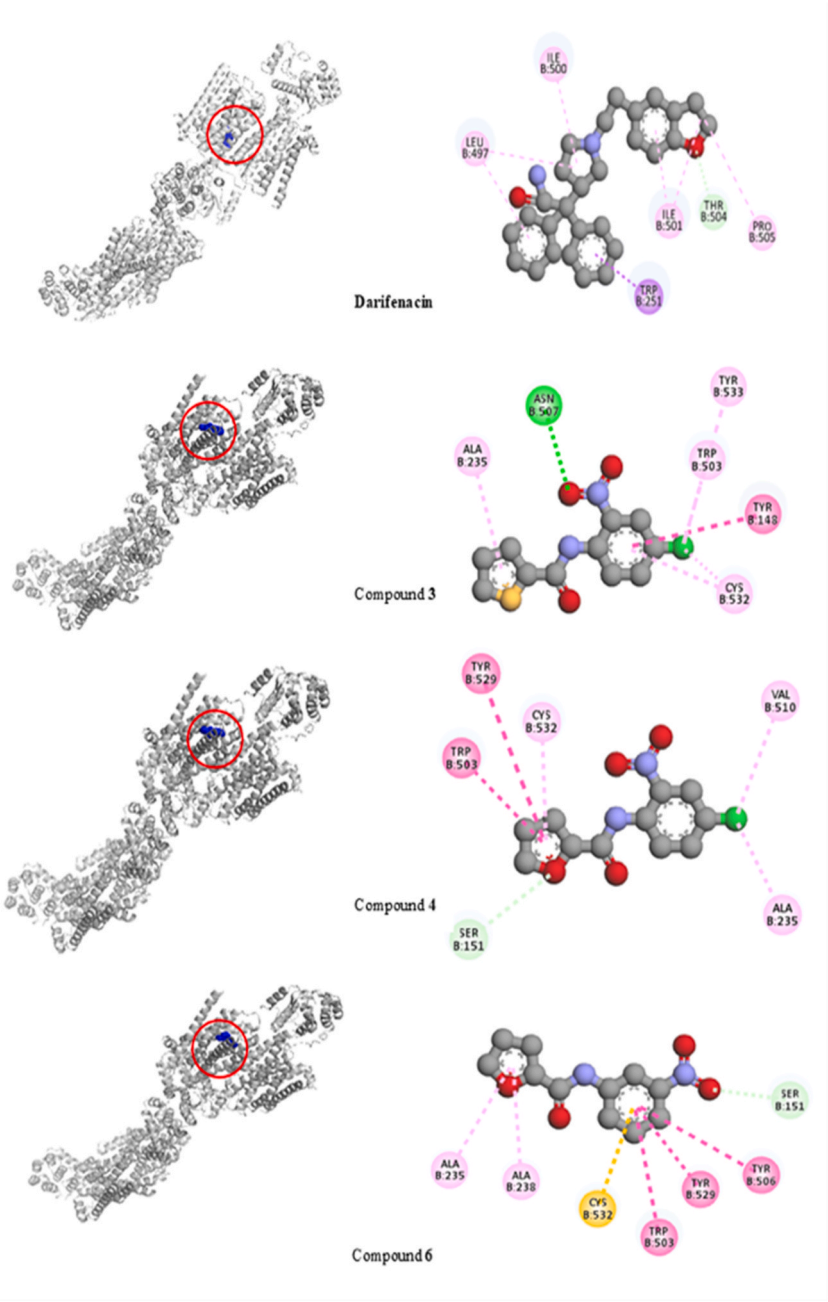

Fig. 6. Interaction between M3 muscarinic receptor with darifenacin, compounds **3**, **4**, and **6.** Green: conventional hydrogen bond, pink-violet: hydrophobic, orange: pi-cation/pi-anion/pi-sulfur, cyan: carbon-hydrogen bond. (For interpretation of the references to colour in this figure legend, the reader is referred to the Web version of this article.)

respectively in the reactions.

As shown in scheme-1 and Table 1, six heteroaryl amide derivatives (Compounds **1**–**6**) were synthesized with good yields (68–85 %) following the procedure described in section 2.2. After purification, characterization was achieved by ^{1}H NMR, ^{13}C NMR, and FT-IR. Experimentally obtained data was compared with previously published literature and the structures of the samples were finally confirmed [32,33].

3.2. Evaluation of analgesic activity

In the case of compounds **1**, **2**, and **4** analgesic activity was observed in a dose-dependent manner. These compounds showed

Table 9
Binding affinity and binding interaction with β-tubulin (PDB ID: 1SA0).

Ligand	Binding Affinity (kcal/mol)	H-bond (Å)	Hydrophobic Interactions and other Interactions
Combrestatin	−6.3	Cys241B (2.74)	Cys241B, Leu255B, Lys254B, Leu248B, Ala250B, Ala316B, Val318B, Lys352B, Ala354B,
1	−6.9	Asp179B (2.02), Cys12B (2.33)	Ser178B, Pro173B, Val171B, ser140B, Gly10B
2	−7.3	Gly144B (2.25), Thr145B (2.53), Asp179B (2.12)	Ser140B, Val171B, Cys12B, Pro173B
3	−6.6	Gly144B (2.52), Asn101B (2.52), asp179B (2.25), Tyr224B (2.94)	Val171B, Pro173B, Cys12B, Ser140B
4	−6.4	Asn258B (2.75)	Leu248B, Ala250B, Leu255B, Met259B, Lys352B
5	−6.0	Ala250B (2.26)	Leu248B, Lys254B, Ala316B, Val318B, Ala354B
6	−6.4	–	Leu248B, Lys352B

considerable analgesic activity ($p < 0.001$) at both low and high doses with writhing inhibition values of 78.97 %, 93.46 %, 77.10 %, 89.72 %, 93.46 %, and 95.79 %, respectively, as compared to standard aceclofenac (91.12 %). Compounds **3** and **5** also demonstrated analgesic activity although they did not show any dose dependency. Compound **6** showed very mild activity. The findings of the writhing inhibition assay have been shown in Table 2.

3.3. Evaluation of anti-inflammatory activity

Compound **4** showed a gradual increase in its anti-inflammatory activity over time. It exerted promising anti-inflammatory activity with 36.9 %, 64.17 %, 82.9 %, and 93.9 % paw edema inhibition at 1st, 2nd, 3rd and 4th hours, respectively. The values were almost similar to that of the standard aceclofenac i.e.: 35.5 %, 78.6 %, 79.3 %, and 91.2 % in 1st, 2nd, 3rd and 4th hours, respectively. For compound **2**, paw inhibition values increased till 3rd hour and showed fall at 4th hour. At, 3rd hour % paw edema inhibition of compound **2** was 93.6 % which was considerably high and statistically significant. Compounds **1** and **3** showed variable activity over time. On the other hand, compounds **5** and **6** did not show encouraging findings. The findings of the analysis are summarized in Table 3.

3.4. Evaluation of cytotoxicity

3.4.1. Brine shrimp lethality bioassay

The LC_{50} for the positive control vincristine sulphate (VS), was determined to be 0.46 μM. Compounds **4, 5,** and **6** showed LC_{50} of 6.34 μM, 2.78 μM and 28.38 μM, respectively concluding noticeable cytotoxicity of these compounds (Fig. 3a) which is comparable to vincristine sulphate. Compounds **1**, **2,** and **3** did not show considerable activity compared to the standard.

3.4.2. Trypan blue dye exclusion test for cytotoxicity

Compounds **1–3** resulted in more than 95 % survival of cells thus indicating their lack of cytotoxicity, whereas, compounds **4–6** showed significant cytotoxic activity with only 10–20 % cell survival upon treatment with the test compounds at 500 μg/ml concentration (Table 4).

3.4.3. MTT assay

MTT assay was carried out for compounds **4–6** which showed promising result in trypan blue dye exclusion test. Compound **5** showed lowest IC_{50} which was 281.96 μM indicating its higher potential to act as cytotoxic agent. Compound **6** was found to possess moderate activity for which IC_{50} was 637.41 μM. Fig. 3b summarizes the findings of MTT assay.

3.5. Evaluation of antidiarrheal activity

Among the synthesized diaryalamides, compounds **5** and **6** showed marked antidiarrheal effects with 85.00 % and 71.67 % inhibition of defecation, respectively, at the dose of 25 mg/kg and 86.67 % and 83.33 %, inhibition, respectively, at the dose of 50 mg/kg. The obtained results are comparable to the standard loperamide (85.00 % inhibition of defection at 25 mg/kg dose). Other compounds showed negligible antidiarrheal properties. Table 5 summarizes the findings of anti-diarrheal activity assay.

3.6. Evaluation of antioxidant activity

In the DPPH assay, ascorbic acid was found to have IC_{50} of 12.38 μM, whereas, synthesized compounds did not show antioxidant potential with IC_{50} ranging from 1022.73 to 141134.42 μM.

3.7. Molecular docking

Molecular docking studies were performed for the all the synthesized compounds. Since our synthesized samples exhibited

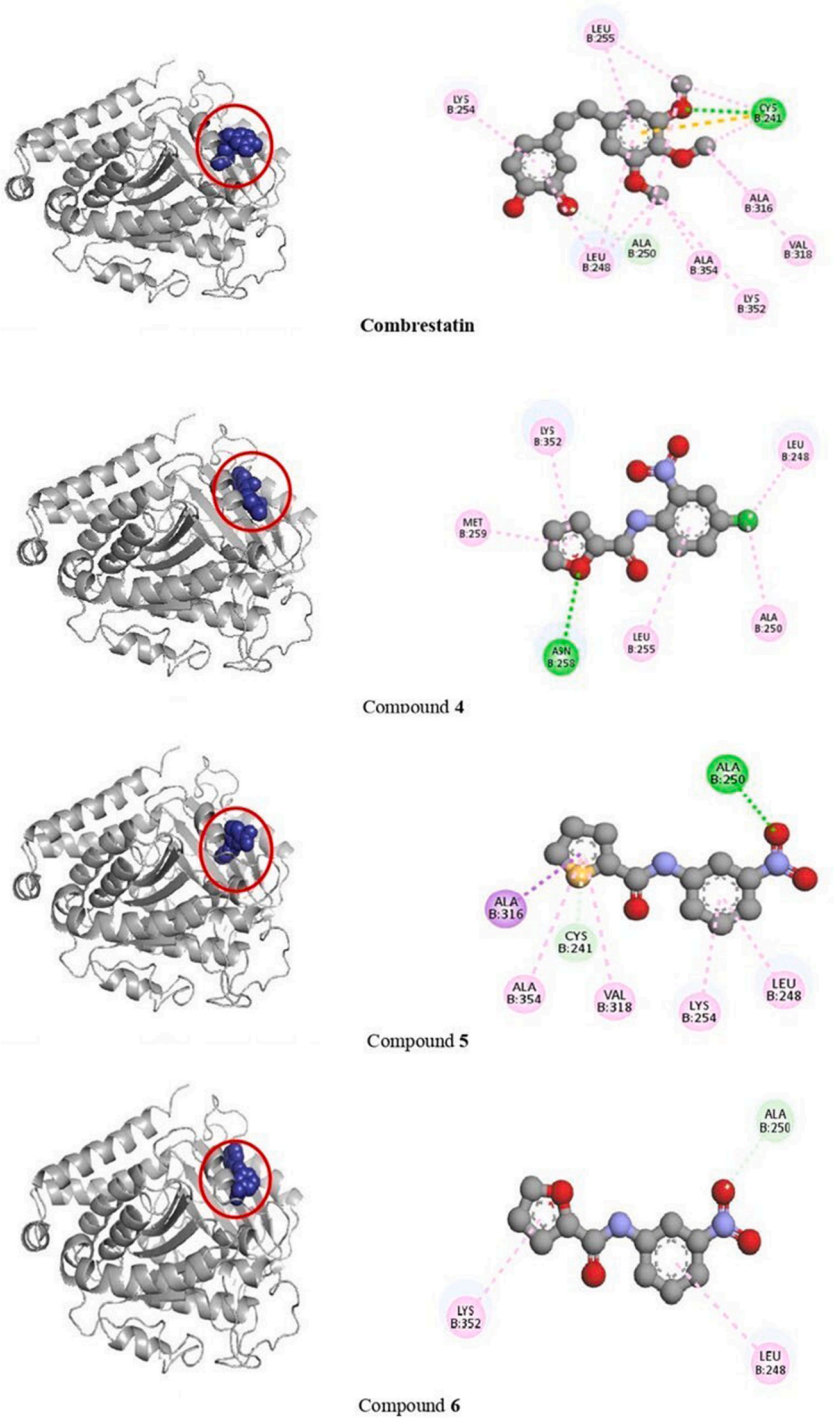

Fig. 7. Interaction between β-tubulin with combrestatin, compounds **4, 5,** and **6**. Green: conventional hydrogen bond, pink-violet: hydrophobic, orange: pi-cation/pi-anion, cyan: carbon-hydrogen bond. (For interpretation of the references to colour in this figure legend, the reader is referred to the Web version of this article.)

potential analgesic, antidiarrheal and cytotoxic effects, *in silico* studies were undertaken for gaining preliminary understanding of their mechanism of action.

Synthesized compounds **1**–**6** and the standard aceclofenac were docked against the target protein cyclooxygenase-2 (COX-2) to investigate if the observed analgesic and anti-inflammatory effect is related to this enzyme. As this enzyme is involved in the formation of prostaglandins that are responsible for mediating pain and also aids inflammatory process. The binding score for aceclofenac was

Table 10
Binding affinity and binding interaction with human topoisomerase-II (PDB ID: 3QX3).

Ligand	Binding affinity (kcal/mol)	H-bond (Å)	Hydrophobic interactions and other interactions
Etoposide	−7.5	Arg820A (2.79)	Tyr820A, Gly 776B, Glu777B, Tyr778B
1	−6.3	Ala768B (2.29)	Phe823A, Lys759A, Ala768B, Glu769B, Val758A
2	−6.4	Ala 769B (2.62)	Phe823A, Lys759A, Ala768B, Glu769B, Val758A
3	−6.0	Ala768B (2.18)	Ala768B, Lys759A, Phe823A, Val758A, Glu769B, Lys759A
4	−5.8	Lys759A (2.76)	Val758A, Ala768B, Glu769B, Phe823A.
5	−6.1	Lys759A (2.06)	Phe823A, Ala768B, Lys759A, Glu769B,
6	−6.6	Gln778A (2.48) Gln778B (2.71)	Ala761A, Gln762A, Arg820A, Ala761B, Arg820B

found to be −7.4 kcal/mol against COX-2, whereas, binding scores for compounds **1**–**6** against COX-2 ranged between −6.4 and −7.8 kcal/mol (Table 6). Binding interactions between aceclofenac and the synthesized compounds with COX-2 are illustrated in Fig. 4 and Fig. S1.

Kappa opioid receptor and M3 muscarinic receptor were exploited for identifying the mechanism underlying antidiarrheal effects of the test samples. All the synthesized compounds showed less binding affinity than standard loperamide as shown in Table 7. Fig. 5 and Fig. S2 outline the binding interactions of standards and compounds **1**–**6** against kappa opioid receptor (PDB ID: 6VI4).

Muscarinic receptor is also involved in gastrointestinal motility thus molecular docking was performed against M3 receptor (PDB ID: 4DAJ). Table 8 and Fig. 6 and Fig. S3 summarize the findings of molecular docking of test compounds **1**–**6** against M3 receptor. Compounds **3**–**6** were found to have strong binding affinity against M3 receptor with scores ranging from −8.0 kcal/mol to −8.1 kcal/mol.

In order to elucidate the mechanism underlying cytotoxicity shown by the synthesized samples molecular docking of the compounds was performed against several targets such as β-tubulin, human topoisomerase II, Src homology, MMP9 and others along with respective control ligands.

The binding affinity of the synthesized compounds ranged between −6.0 kcal/mol to −7.3 kcal/mol, compared to −6.3 kcal/mol of combrestatin against β tubulin. The binding affinities and interactions for the compounds against β-tubulin are shown in Table 9 and binding interactions are presented in Fig. 7.

The binding affinities of the synthesized compounds were comparatively less than that of control ligand etoposide and among the synthesized compounds compound **6** (Table 10) showed highest affinity towards human topoisomerase II (PDB ID 3QX3) The binding interactions of the compounds are shown in Fig. 8**.**

When docked against another anticancer target Src kinase, compound **5** showed highest binding affinities among the synthesized samples with a value of −7.9 kcal/mol, however, all compounds showed less affinity than the standard dasatinib (Table 11 and Fig. 9).

Research is still going on for development of a suitable inhibitor against PPAR-γ. The binding interaction and affinities of synthesized samples **1**–**6** are given in Table 12 and Fig. 10. Experimental inhibitor 14R was taken into consideration to compare the obtained results. The binding affinities of samples ranged beteween −7.2 kcal/mol to −7.4 kcal/mol whereas 14R showed highest binding affinity (−8.9 kcal/mol).

MMP9 is a prospective target in the prognosis of cancer thus it was taken under consideration for molecular docking analysis. Compounds **4**, **5** and **6** have shown promising result in *in silico* analysis. Binding affinity of compound **5** was equal to the experimental inhibitor N73 of MMP9 and compound **6** was greater than that of N73 with a value of −9.1 kcal/mol. Binding interaction and binding affinities of test and standard compounds against MMP9 are shown in Fig. 11 and Table 13, respectively.

3.8. In silico ADME/T prediction

Pharmacokinetic properties of drugs have an intimate relation with the physicochemical nature of drug molecule. Current approaches in drug development are focused towards designing molecules which have favorable pharmacokinetic properties which will in turn facilitate the drugs action inside the body. In terms of identifying lead molecule, ADME and toxicological evaluation of target entity is an important factor [34]. All pharmacokinetic data of the synthesized samples are presented in Table 14.

4. Discussion

Overall, six heteroaryl amide derivatives were synthesized using condensation reaction between acid chlorides and heteroaryl amines in good yields (68–85 %). Spectroscopic methods were exploited for the characterization purpose. Pharmacological screening for analgesic, anti-inflammatory, antidiarrheal, antioxidant as well as cytotoxic potential was performed. The tested compounds exhibited activities which ranged from mild to significant in cases of analgesic, anti-inflammatory, anti-diarrheal, and cytotoxic effects. However, the synthesized samples lacked antioxidant activity.

Compounds **1**–**5** exhibited promising analgesic activity compared to the standard aceclofenac. COX-2 was selected as target for *in silico* analysis as this enzyme is involved in the cyclooxygenase pathway responsible for mediation of pain and inflammation [35]. The findings of the *in silico* study revealed that, all the synthesized derivatives exhibited comparable binding affinities similar to that of standard aceclofenac. Despite the fact that, compound **6** did not possess any analgesic or anti-inflammatory activity *in vivo*, its binding scores against COX-2 were considerable. This ambiguity maybe attributed to several factors. Previously it was found that, the higher

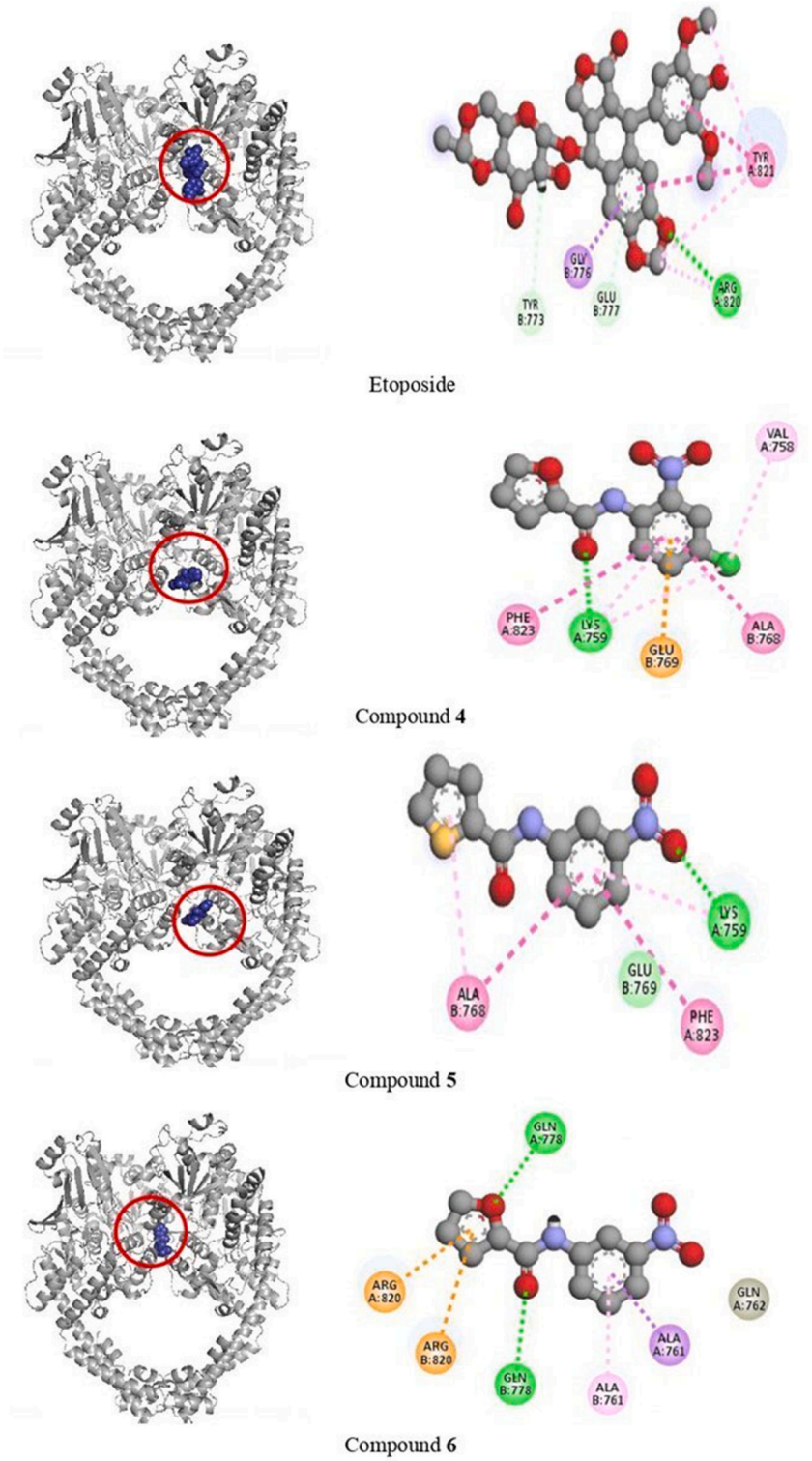

Fig. 8. Interaction between human topoisomerase IIb with etoposide, compounds **4**, **5,** and **6**. Green: conventional hydrogen bond, pink-violet: hydrophobic, orange: pi-cation/pi-anion, cyan: carbon-hydrogen, grey: van-daar waals bond. (For interpretation of the references to colour in this figure legend, the reader is referred to the Web version of this article.)

Table 11
Binding affinity and binding interaction with Src kinase (PDB ID: 2H8H).

Ligand	Binding affinity (kcal/mol)	H-bond (Å)	Hydrophobic interactions and other interactions
Dasatinib	−8.7	Tyr340A (1.88), Lys401A (2.89), Gln251A (2.09)	Ser342A, Glu239A, Val399A, Leu161A, Arg318A, Tyr340A
1	−7.2	Asp404A (2.45)	Val281A, Lys295A, Ala403A, Asp404A. Leu325A, Val323A
2	−7.6	Asp404A (2.08)	Val281A, Lys295A, Ala403A. Leu325A, Val323A
3	−6.4	–	Val281A, Lys295A, Ala403A. Leu393A, Asp404A, Ala390A, Ile336A
4	−6.7	Asn397A (2.46), Ser248A (2.29), Glu396A (2.17, 2.19)	Val399A, Gly395A, Glu396A
5	−7.9	Thr338A (2.46), Phe405A (2.54)	Leu393A, Ala293A, Val281a, Asp404A, Ala403A, Lys295A, Ile336A
6	−6.3	Gln251A (2.23), Lys401A (2.24)	Arg318A

the number of residues involved in hydrophobic interactions, the higher would be the stability of the complex and presence of polar residues increased the chance of positioning the ligand at the target site [36]. Another major factor is shorter hydrogen bonds tends to be stronger and hydrogen bond less than 2.3 Å are particularly important [37,38]. The only hydrogen bond with His207A in the interaction of compound **6** with COX-2 is 2.74 Å long and no polar residues were found to be involved in the process. The 2D diagram of protein ligand complex showed that, a total of three amino acids i.e. His207A, Ala202A and Gln203A were involved in the overall interaction. For the remaining five samples, the total number of amino acids of target protein responsible for interaction was higher and among them compounds **2** and **3** involved interactions with polar amino acid residues. The hydrogen bond length was shorter in majority of cases. The mentioned factors might have attributed to the instability of the compound **6**-COX 2 complex which resulted in failure of *in vivo* analgesic and anti-inflammatory activity.

Although some of the synthesized samples have shown a gradual increase in their anti-inflammatory effects with time but most of them showed variable responses over time. The anti-inflammatory effect given by compound **4** can be considered the most promising among the six synthesized compounds. Recently, several heteroarylamide derivatives have been found to possess promising cyclo-oxygenase inhibitory activity in both *in vitro* and *in silico* studies [39,40]. Some of the previously synthesized carboxamides have been found to be associated with both analgesic and anti-inflammatory effects by targeting COX-2 which was confirmed by *in vivo, in vitro* and *in silico* studies [41,42]. Thus, considering the findings of the current study along with previously published literatures we can assume COX inhibition as a probable mechanism for the analgesic and anti-inflammatory effects exerted by the synthesized compounds.

None of the synthesized samples showed considerable antioxidant activity. Previously it was believed that, anti-oxidant activity and anti-inflammatory activity were related. Reactive oxygen species (ROS) can result in certain type of injuries at cellular level, which may cause or propagate inflammation by activating genes related to cytokines and adhesion molecules [43]. Thus, antioxidants can indirectly reduce inflammation. On the other hand, inflammation gives rise to ROS by activating cGAS/STING pathway, so, by treating inflammation, oxidative stress may be reduced [44]. However, recently it was identified that, it might not be the case i.e. anti-inflammatory activity may not always be associated with anti-oxidant effects and vice versa [45].

GI opioid receptors as well as muscarinic receptor (M3) make substantial contribution in maintenance of peristaltic motion and are thus, opioid receptor agonists and muscarinic receptor antagonists are associated with anti-diarrheal effects [46–49]. Among the synthesized samples, compounds **5,** and **6** showed comparable antidiarrheal activity to that of standard loperamide when tested *in vivo*. In the molecular docking studies against kappa opioid receptor, the binding score for loperamide was −9.2 kcal/mol which was highest of all, whereas, the synthesized samples possessed binding scores ranging from −6.6 to −7.6 kcal/mol. On the other hand, darifenacin was taken as the standard to compare the binding affinities of the synthesized compounds against M3 muscarinic receptor. Darifenacin is an FDA approved drug which shows selectivity and competitive inhibition towards M3 muscarinic receptor [50]. Compounds **3–6** showed higher binding affinities towards M3 receptor than darifenacin. The binding affinity of the control molecule darifenacin was −7.7 kcal/mol, whereas, synthesized compounds showed binding affinities ranging from −7.3 kcal/mol to −8.1 kcal/mol. Compounds **3** and **4** had binding score of −8.1 kcal/mol and compounds **5** and **6** had equal binding affinity of −8.0 kcal/mol. The docking scores against both kappa and muscarinic receptors reflect the findings of *in vivo* assay. In both cases compounds **3–6** showed promising results whereas compounds **1** and **2** neither showed good binding score nor *in vivo* antidiarrheal activity. The synthesized compounds showed greater affinity towards M3 receptor than kappa receptor, suggesting that their mechanism of action might be different from that of loperamide. Furthermore, some synthesized carboxamide derivatives, as reported in previous studies, have shown potent M3 antagonistic activity which coincides with our findings of both *in vivo* and *in silico* studies [51,52].

Three of the synthesized samples, compounds **4, 5,** and **6** have shown promising result in brine shrimp lethality bioassay and trypan blue dye exclusion test with only 10–20 % cell viability when tested on HeLa cell Line. MTT assay revealed IC_{50} of mentioned compounds ranging between 281.96 and 1410.14 μM. Among these, compound **5** has the lowest IC_{50} which makes it the most potent cytotoxic agent of the tested samples. According to the recent studies, tubulin polymerization has been inhibited by the use of different carboxamide derivatives [53–56]. Some of the reported works suggest that carboxamides interact with tubulin in their colchicine binding site [57]. Human topoisomerase-II is also an important target for synthesized carboxamide derivatives according to extensive literature review [58]. Nitazoxanide is an antiprotozoal medication which have been extensively studied for its anticancer activity

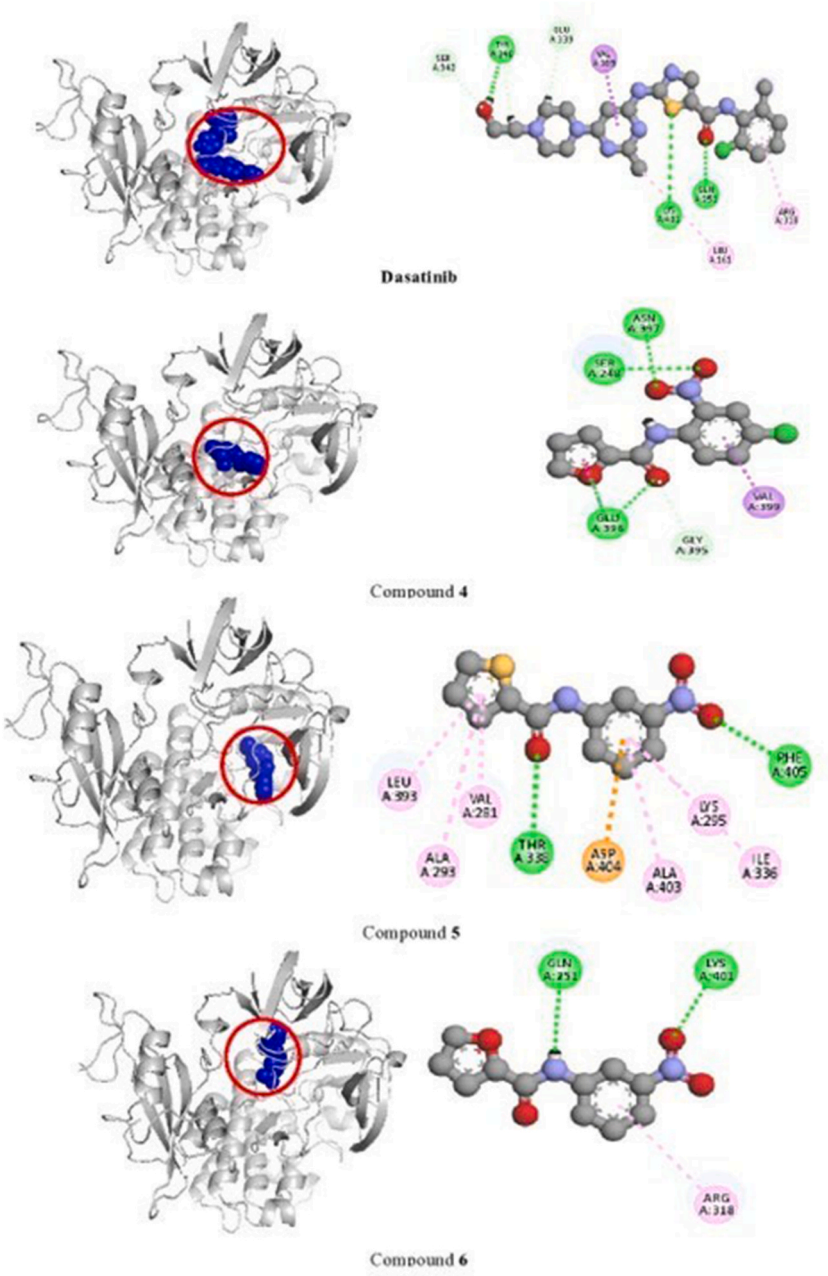

Fig. 9. Interaction between human Src with dasatanib, compounds **4**, **5,** and **6**. Green: conventional hydrogen bond, pink-violet: hydrophobic, orange: pi-cation/pi-anion, cyan: carbon-hydrogen, grey: van-daar waals bond, purple: pi-sigma. (For interpretation of the references to colour in this figure legend, the reader is referred to the Web version of this article.)

against several types of cancer. Not only nitazoxanide but also some of its derivatives have shown considerable affinity towards MMP9, Src homology and PPAR-γ in *in silico* study [5,59,60]. As our synthesized compounds share close structural resemblance with nitazoxanide analogs, these three targets were also considered for understanding the probable mechanism responsible for cytotoxicity. Moreover, the chosen targets have been associated with several types of cancers, for example, human topoisomerase II is associated with ovarian cancer, Src homology and MMP9 has been found to be associated with pancreatic cancer [61–63]. On the other hand, PPAR-γ upregulation is associated with prostatic cancer [64]. Microtubules and its associated proteins have been found to play key a role in stress responses at cellular levels which in turn increases the survivability of the cancer cells [65]. Therefore, these five targets were chosen for molecular docking analysis.

Combrestatin is a drug which acts by inhibiting β-tubulin and it was chosen for comparing the binding affinities of our samples with β-tubulin. Binding affinity of combrestatin was −6.3 kcal/mol, whereas, binding affinity of compound **4** and **6** was −6.4 kcal/mol and

Table-12
Binding affinity and binding interaction with PPAR-γ (PDB ID: 4HEE).

Ligand	Binding affinity (kcal/mol)	H-bond (Å)	Hydrophobic interactions and other interactions
14R	−8.9	Ile326X (2.96)	Ile326X, Ala292X, Leu330X, Lys367X, Met364X, Cys285X, Ile341X, Ser342X, Leu228X, Pro227X, Arg288X
1	−7.0	Arg288X (2.55), Cys285X (1.82)	Arg288X, Cys285X, Ala292X, Leu330X, Ile326X, Lys367X, Phe363X
2	−7.3	–	Cys285X, Arg288X, Leu530X, Ile326X, Lys367X
3	−6.9	Arg288X (2.24)	Leu228X, Leu333X, Arg288X, Ile326X, Ala292X, Leu330X
4	−7.2	Cys285X (2.23)	Cys285X, Phe363X, Ser289X, Val339X, Leu333X, Arg288X, Leu330X
5	−7.3	Cys285X (2.37)	Cys285X, Phe363X, Ser289X, Val119X, Leu333X, Arg288X, Leu330X
6	−7.4	Cys285X (2.00), Arg288X (3.85)	Cys285X, Arg288X, Leu330X, Phe363X

compound **5** was −6 kcal/mol. Despite having the lowest binding affinity towards target protein, compound **5** exerted cytotoxicity on cell line. This can probably be explained that compound **5** formed a hydrogen bond with bond length shorter than 2.3 Å. The short bond length contributes to pronounced activity in the biological system [66]. Another, explanation could be that compound **5** functions through another target molecule more prominently.

In case of *in silico* studies against human topoisomerase-II, etoposide was chosen as standard, and it was found that the binding affinity of etoposide was −7.5 kcal/mol, whereas, all other synthesized compounds showed lesser binding affinities than this, predicting that this might not be a target of the synthesized compounds. Similarly, docking with Src kinase and PPAR-γ, where dasatinib and an experimental inhibitor 14R were used as standards, yielded negative results with synthesized compounds having much less affinity towards the targets than the aforementioned standard molecules. However, since docking results may sometimes vary due to difference of conditions compared to biological systems, further *in vivo* and *in vitro* experiment is required.

MMP9 is an important driver of tumorigenesis for which no ideal inhibitor has been identified due to diversified reasons [67]. N73 is an experimental inhibitor to MMP9 which was considered as standard for current simulation [68]. Interestingly, compound **5** and N73 both showed similar binding affinities of −8.8 kcal/mol towards MMP9 and compound **6** showed the highest binding score of −9.1 kcal/mol. It is evident that compound 5 and 6 showed strong affinity towards MMP9 suggesting that it can be a target macromolecule of these compounds, yet further *in vivo*, *in vitro* and more *in silico* experiments are required to confirm these results.

There is a plethora of macromolecules that participate in cancer development. According to some literature carboxamides have been identified to have effect against VEGFR2, MAPK1 protein kinase and CDK/A2 [69,70]. Some other amide based drugs like niclosamide, nitazoxanide, mebendazole showed anticancer effects by interacting with m-Tor and hedgehog pathways [5,71,72]. *In silico* analysis of the compounds **4**–**6** was also accomplished against some other proteins associated to cancer i.e. MEK1, and MEK 2, MAPK, and DFFR. Although the results were unsatisfactory. So, to establish the exact mechanism underlying cytotoxic effects of compounds **4, 5, 6** further experiments involving different cell lines and animal models are necessary.

Although it is difficult to deduce a precise structure activity relationship (SAR) based on limited number of derivatives, the SAR of the synthesized samples was assumed on the basis of the position and nature of the substituents on the phenyl ring.

The synthesized compounds contain nitro and chloride substituents (Fig. 12a–c) on the phenyl ring. The compounds also contain thiophene or furan ring as heteroaryl moiety. In the case of thiophene derivatives, placement of nitro group at *ortho*, *meta* and *para* positions did not affect analgesic activity greatly. However, in the case of furan derivatives when nitro group was placed at *meta* position (Compound **6**), analgesic activity reduced remarkably. Chloro-substituent at *para* position enhanced both analgesic and anti-inflammatory activity (Fig. 12**c**). Thus, 2-nitro-4-chhlorophenyl derivatives (compounds **3** and **4**) showed highest anti-inflammatory as well as analgesic activity among the synthesized analogs. This might be due to significant halogen hydrophobic interactions as seen in docking study.

The presence of -NO_2 group at the *meta* position of the phenyl ring (Fig. 12**b**) increases antidiarrheal activity irrespective of the heteroaryl moiety (compounds **5** and **6**). When the -NO_2 group is shifted to *para* position of the phenyl ring (Fig. 12**a**), antidiarrheal activity is greatly reduced (compounds **1** and **2**). These results are supported by molecular docking study, where compounds **5** and **6** showed greater binding affinity than compound **1** and **2**. This observation may be explained as electron withdrawing effect of -NO_2 group is more pronounced at *para* position than *meta* position resulting more availability of pi electrons at the aromatic ring with *meta* substituent which might have led to stronger hydrophobic interactions. Introduction of -Cl group, which is also a deactivating group, at *para* position and shifting -NO_2 group at *ortho* position of the benzene ring shows moderate anti-diarrheal activity. However, to draw any definite conclusion and evaluate the role of -Cl and -NO_2 group more derivatives need to be synthesized.

Compounds with -NO_2 group at the *meta* position of the phenyl ring provide greater cytotoxic ability to the synthesized samples **5** and **6** compared to *para* substituted compounds **1** and **2**. Furan containing 2-nitro-4-chhlorophenyl derivative compound **4** also exhibited cytotoxicity. However, complexity of anticancer drug mechanism impedes development of precise SAR and warrants further synthesis of analogs along with determination of specific target macromolecule with detailed studies.

According to Lipinski's rule of five, for a drug to be a good candidate for oral route must have molecular parameters within a specific range. These parameters include molecular weight less than 500 Da, total number of hydrogen bond donors $\leq$5, the total number of hydrogen bond acceptors $\leq$10, octanol-water partition ratio (LogP) $<$ 5, molar refractivity ranging from 40 to 130 [73]. All six synthesized samples pass the criteria of Lipinski's rule of Five.

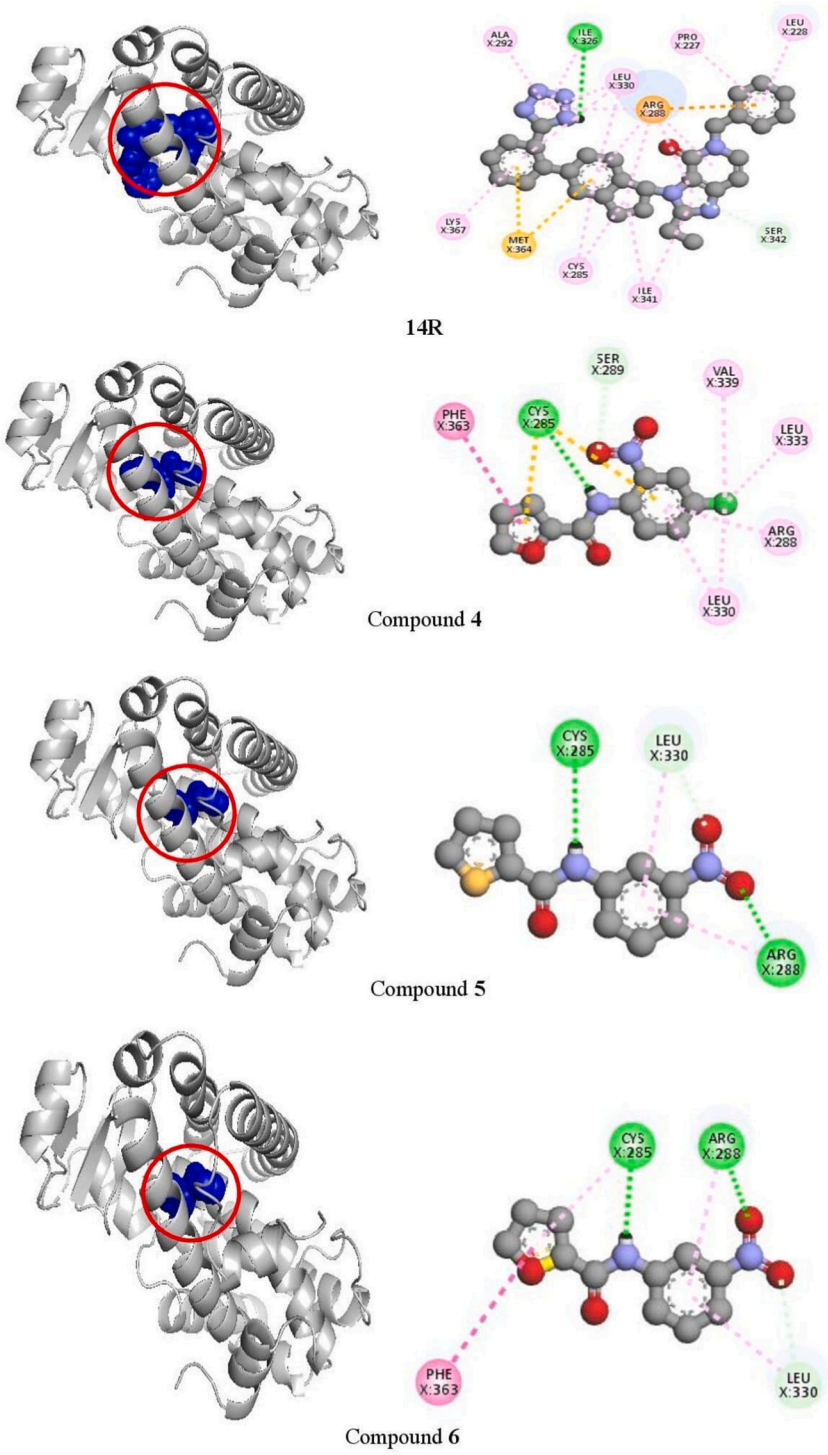

Fig. 10. Interaction between human PPAR-γ with 14R, compounds **4**, **5,** and **6**. Green: conventional hydrogen bond, pink-violet: hydrophobic, orange: pi-cation/pi-anion, cyan: carbon-hydrogen, grey: van-daar waals bond, purple: pi-sigma. (For interpretation of the references to colour in this figure legend, the reader is referred to the Web version of this article.)

Caco-2 permeability is a measure which provides insights about a drugs permeability and absorption through the intestinal membrane when taken orally [74]. Our synthesized compounds have shown acceptable values in terms of both human intestinal absorption and human intestine colon cancer cell (caco2) permeation values. All six derivatives (**1–6**) were predicted to have very high

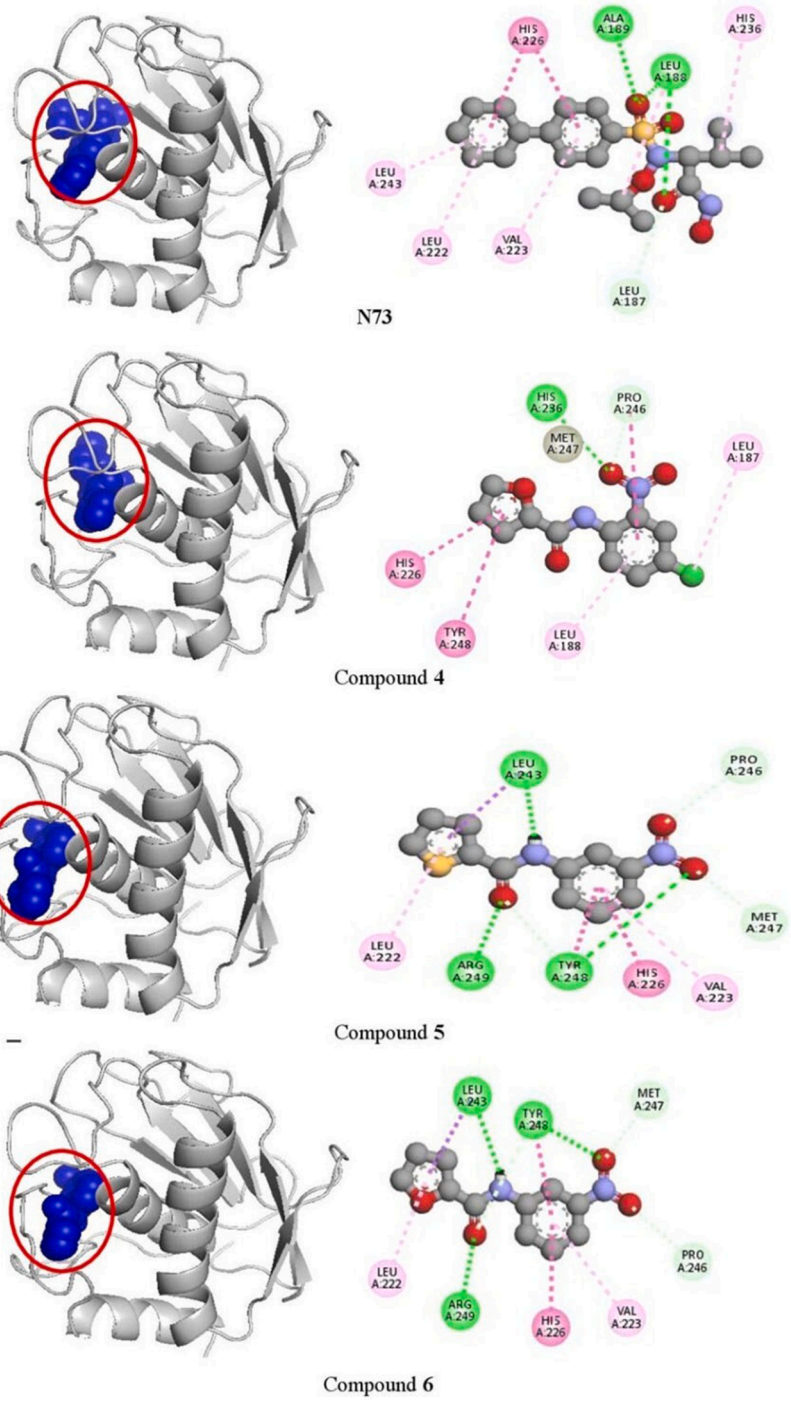

Fig. 11. Interaction between human MMP9 with N73, compounds **4**, **5,** and **6**. Green: conventional hydrogen bond, pink-violet: hydrophobic, orange: pi-cation/pi-anion, cyan: carbon-hydrogen, grey: van-daar waals bond, purple: pi-sigma. (For interpretation of the references to colour in this figure legend, the reader is referred to the Web version of this article.)

Table 13
Binding affinity and binding interaction with matrix metalloproteinase 9 (MMP9) (PDB ID: 4XCT).

Ligand	Binding affinity (kcal/mol)	H-bond (Å)	Hydrophobic interactions and other interactions
N73	−8.8	Ala189A (2.52) Leu228A (2.17)	His226A, Leu243A, Leu222A, Val223A, Leu187A, His236A, Leu228A
1	−7.5	Leu288A (2.04)	Leu288A, Val223A, His226A
2	−7.6	Arg249A (1.94)	Arg249A, Met247A, Val223A, His226A, Tyr248A
3	−6.9	Ala189A (2.25), Pro246A (2.55)	His236A, Leu188A, Tyr248A, Val223A, Met247A, Glu227A. His226A
4	−7.3	His236A (2.70)	Leu187A, Pro246A, Leu288A, Tyr248A, Leu243A, His226A, Met247A
5	−8.8	Leu243A (2.38), Arg249A (2.31), Tyr248A (2.21, 3.85)	Leu222A, Pro246A, Met247A, Val223A, His226A, Leu243A
6	−9.1	Leu243A (2.28), Arg249A (2.25), Tyr248A (2.59)	Leu222A, Met247A, Pro246A, His26A, Val223A, Leu243A, Tyr248A

Table 14
ADME, physicochemical and toxicological properties of synthesized compounds.

Physicochemical and ADMET properties	Compound					
	1	2	3	4	5	6
Molecular weight	248.26	232.19	282.71	266.64	248.26	232.19
LogP	1.96	2.44	3.56	1.96	2.02	1.29
H-bond acceptor	3	4	4	4	4	4
H-bond donor	1	1	1	1	1	1
Molar refractivity	67.36	61.74	72.37	66.75	67.37	61.74
Human intestinal absorption	+0.9348	+0.8939	+0.9558	+0.9295	+0.9303	+0.8883
Caco-2 permeability	+0.8213	+0.8336	+0.6734	+0.669	+0.8324	+0.7724
Blood brain barrier	+0.7750	+0.6500	+0.800	+0.9295	+0.7750	+0.6750
CYP 1A2 Inhibition	+	+	+	+	+	+
CYP 2C19 inhibition	−	−	+	+	−	−
CYP 2C9 inhibition	−	−	+	−	−	−
CYP 2C9 substrate	−	−	−	−	−	−
CYP 2D6 inhibition	−	−	−	−	−	−
CYP 2D6 substrate	−	−	−	−	−	−
CYP 3A4 inhibition	−	−	−	−	−	−
CYP 3A4 substrate	−	+	+	+	−	+
p-glycoprotein inhibitor	−	−	−	−	−	−
p-glycoprotein substrate	−	−	−	−	−	−
Carcinogenicity	−	−	+	+	−	−

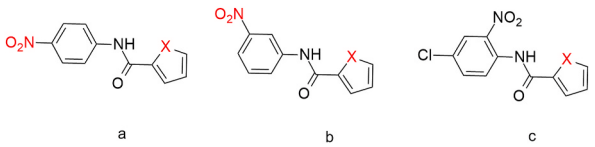

Fig. 12. Elucidation of Stricture activity relationship (SAR) (when X = S, a = compound **1**, b = compound **3**, c = compound **5**; when X = O, a = compound **2**, b = compound **4**, c = compound **6)**.

human intestinal absorption values (+0.8883 to +0.9558) and satisfying caco2 permeability (+0.6734 to +0.9348).

Cytochrome enzymes are important regulators of metabolism for drugs and other chemical substances. From the ADME/T prediction, most of the synthesized samples were identified to be substrates for CYP3A4. However, all the compounds were predicted to be associated with CYP1A2 enzyme inhibition. The compounds were neither substrate nor inhibitor of P-gp, which is considered to be able to efflux drugs from cells.

5. Conclusion

Six heteroaryl amide derivatives have been synthesized successfully in good yields and they were investigated for their pharmacological effects. Compounds **1**–**5** showed promising peripheral analgesic effect, compound **5** and **6** had notable antidiarrheal effect and **4**–**6** showed significant cytotoxic properties with compound **5** being most potent with lowest IC_{50}. Molecular docking analysis confirmed the findings of *in vivo* and *in vitro* analysis. *In silico* ADMET analysis revealed that the synthesized compounds possessed

properties conducive to drug development. Thus, it can be concluded that our synthesized compounds hold potential to be developed as potent therapeutic agents.

CRediT authorship contribution statement

Nazifa Tabassum: Writing – original draft, Investigation, Formal analysis, Data curation. **Sabiha Enam Spriha:** Writing – review & editing, Writing – original draft, Methodology, Investigation. **Poushali Saha:** Methodology, Formal analysis. **Fahad Imtiaz Rahman:** Project administration, Methodology, Formal analysis. **ASM Monjur Al Hossain:** Writing – review & editing, Project administration. **S. M. Abdur Rahman:** Writing – review & editing, Supervision, Funding acquisition, Conceptualization.

Ethics statement

The study was conducted according to the guidelines of the Declaration of Helsinki, and approved by the Ethical Review Committee of the Faculty of Biological Sciences, University of Dhaka (approval number: 208/Biol Scs and date of approval: December 20, 2022).

Data availability

All the relevant data associated with present research has been enclosed in the manuscript and supplementary file.

Funding

The project was funded by Dhaka University Centennial Research Grant.

Declaration of competing interest

The authors declare that they have no known competing financial interests or personal relationships that could have appeared to influence the work reported in this paper.

Acknowledgements

The authors express their heartfelt gratitude to Dhaka University Centennial Research Grant for the financial aid and Chemical Biology and DNA Research Lab, Dhaka University, where all the research work was carried out.

Appendix A. Supplementary data

Supplementary data to this article can be found online at https://doi.org/10.1016/j.heliyon.2024.e40630.

References

[1] J.-F. Rossignol, Nitazoxanide: a first-in-class broad-spectrum antiviral agent, Antivir. Res. 110 (2014) 94–103, https://doi.org/10.1016/j.antiviral.2014.07.014.
[2] S. Anshul, R.B. Hans, K.G. Surajit, Update on nitazoxanide: a multifunctional chemotherapeutic agent, Curr. Drug Discov. Technol. 15 (2018) 201–213.
[3] N. Di Santo, J. Ehrisman, A functional perspective of nitazoxanide as a potential anticancer drug, Mutat. Res. Mol. Mech. Mutagen. 768 (2014) 16–21, https://doi.org/10.1016/j.mrfmmm.2014.05.005.
[4] S.M. Abdur Rahman, T. Ahmed, M. Asaduzzaman, F.I. Rahman, A.K.A. Chowdhury, Broad spectrum antimicrobial, anti-inflammatory and peripheral analgesic activities of heteroaryl nitazoxanide analogs, Egypt, Pharm. J. 23 (2024) 348, https://doi.org/10.4103/epj.epj_218_23.
[5] T. Ahmed, S.M.A. Rahman, M. Asaduzzaman, A.B.M.M.K. Islam, A.K.A. Chowdhury, Synthesis, in vitro bioassays, and computational study of heteroaryl nitazoxanide analogs, Pharmacol. Res. Perspect. 9 (2021) e00800, https://doi.org/10.1002/prp2.800.
[6] X. He, L. Zhu, S. Li, Z. Chen, X. Zhao, Loperamide, an antidiarrheal agent, induces apoptosis and DNA damage in leukemia cells, Oncol. Lett. 15 (2017) 765, https://doi.org/10.3892/ol.2017.7435.
[7] L. Chen, H. Deng, H. Cui, J. Fang, Z. Zuo, J. Deng, Y. Li, X. Wang, L. Zhao, Inflammatory responses and inflammation-associated diseases in organs, Oncotarget 9 (2017) 7204–7218, https://doi.org/10.18632/oncotarget.23208.
[8] M.S. Jan, S. Ahmad, F. Hussain, A. Ahmad, F. Mahmood, U. Rashid, O.-R. Abid, F. Ullah, M. Ayaz, A. Sadiq, Design, synthesis, *in-vitro, in-vivo* and *in-silico* studies of pyrrolidine-2,5-dione derivatives as multitarget anti-inflammatory agents, Eur. J. Med. Chem. 186 (2020) 111863, https://doi.org/10.1016/j.ejmech.2019.111863.
[9] G. Ali, N.U. Islam, M. Qaim, R. Ullah, M.S. Jan, K. Shabbiri, M. Shafique, M. Ayaz, 2-Hydroxybenzohydrazide as a novel potential candidate against nociception, inflammation, and pyrexia: in vitro, in vivo, and computational approaches, Inflammopharmacology 32 (2024) 643–656, https://doi.org/10.1007/s10787-023-01356-0.
[10] S. Harirforoosh, F. Jamali, Renal adverse effects of nonsteroidal anti-inflammatory drugs, Expet Opin. Drug Saf. 8 (2009) 669–681, https://doi.org/10.1517/14740330903311023.
[11] V.R. Shanbhag, A. Michael Crider, R. Gokhale, A. Harpalani, R.M. Dick, Ester and amide prodrugs of ibuprofen and naproxen: synthesis, anti-inflammatory activity, and gastrointestinal toxicity, J. Pharm. Sci. 81 (1992) 149–154, https://doi.org/10.1002/jps.2600810210.
[12] A.S. Kalgutkar, A.B. Marnett, B.C. Crews, R.P. Remmel, L.J. Marnett, Ester and amide derivatives of the nonsteroidal antiinflammatory drug, indomethacin, as selective cyclooxygenase-2 inhibitors, J. Med. Chem. 43 (2000) 2860–2870, https://doi.org/10.1021/jm000004e.

[13] A.R. Abduelkarem, H.S. Anbar, S.-O. Zaraei, A.A. Alfar, O.S. Al-Zoubi, E.G. Abdelkarem, M.I. El-Gamal, Diarylamides in anticancer drug discovery: a review of pre-clinical and clinical investigations, Eur. J. Med. Chem. 188 (2020) 112029, https://doi.org/10.1016/j.ejmech.2019.112029.

[14] W. Chen, R.A. Mook, R.T. Premont, J. Wang, Niclosamide: beyond an antihelminthic drug, Cell. Signal. 41 (2018) 89–96, https://doi.org/10.1016/j.cellsig.2017.04.001.

[15] S. Saikia, M. Bordoloi, Molecular docking: challenges, advances and its use in drug discovery perspective, Curr. Drug Targets 20 (2019) 501–521, https://doi.org/10.2174/1389450119666181022153016.

[16] A.R. Issahaku, E.Y. Salifu, C. Agoni, M.I. Alahmdi, N.E. Abo-Dya, M.E.S. Soliman, M. Rudrapal, N. Podila, Discovery of potential KRAS-SOS1 inhibitors from South African natural compounds: an in silico approach, ChemistrySelect 8 (2023) e202300277, https://doi.org/10.1002/slct.202300277.

[17] A.R. Issahaku, N. Mukelabai, C. Agoni, M. Rudrapal, S.M. Aldosari, S.G. Almalki, J. Khan, Characterization of the binding of MRTX1133 as an avenue for the discovery of potential KRASG12D inhibitors for cancer therapy, Sci. Rep. 12 (2022) 17796, https://doi.org/10.1038/s41598-022-22668-1.

[18] S.C. Raka, A. Rahman, F. Hussain, S.M.A. Rahman, Synthesis, characterization and in vitro, in vivo, in silico biological evaluations of substituted benzimidazole derivatives, Saudi J. Biol. Sci. 29 (2021) 239, https://doi.org/10.1016/j.sjbs.2021.08.082.

[19] F. Hussain, F.I. Rahman, P. Saha, A. Mikami, T. Osawa, S. Obika, S.M.A. Rahman, Synthesis of sugar and nucleoside analogs and evaluation of their anticancer and analgesic potentials, Molecules 27 (2022) 3499, https://doi.org/10.3390/molecules27113499.

[20] S. Ahmad, M.H. Mahnashi, B.A. Alyami, Y.S. Alqahtani, F. Ullah, M. Ayaz, M. Tariq, A. Sadiq, U. Rashid, Synthesis of michael adducts as key building blocks for potential analgesic drugs: in vitro, in vivo and in silico explorations, Drug Des. Dev. Ther. 15 (2021) 1299–1313, https://doi.org/10.2147/DDDT.S292826.

[21] C.A. Winter, E.A. Risley, G.W. Nuss, Carrageenin-induced edema in hind paw of the rat as an assay for antiiflammatory drugs, Proc. Soc. Exp. Biol. Med. Soc. Exp. Biol. Med. N. Y. N 111 (1962) 544–547, https://doi.org/10.3181/00379727-111-27849.

[22] S.E. Spriha, F.I. Rahman, S.M.A. Rahman, Synthesis, in vivo and in silico analgesic and anti-inflammatory studies of α-D-ribofuranose derivatives, Saudi Pharm. J. SPJ Off. Publ. Saudi Pharm. Soc. 29 (2021) 981–991, https://doi.org/10.1016/j.jsps.2021.07.017.

[23] M.M. Billah, R. Islam, H. Khatun, S. Parvin, E. Islam, S.A. Islam, A.A. Mia, Antibacterial, antidiarrhoeal, and cytotoxic activities of methanol extract and its fractions of Caesalpinia bonducella (L.) Roxb leaves, BMC Compl. Alternative Med. 13 (2013) 101, https://doi.org/10.1186/1472-6882-13-101.

[24] B.A. Avelar-Freitas, V.G. Almeida, M.C.X. Pinto, F.a.G. Mourão, A.R. Massensini, O.A. Martins-Filho, E. Rocha-Vieira, G.E.A. Brito-Melo, Trypan blue exclusion assay by flow cytometry, Braz. J. Med. Biol. Res. Rev. Bras. Pesqui. Medicas E Biol. 47 (2014) 307–315, https://doi.org/10.1590/1414-431X20143437.

[25] W. Strober, Trypan blue exclusion test of cell viability, Curr. Protoc. Im. 111 (2015) A3.B.1–A3.B.3, https://doi.org/10.1002/0471142735.ima03bs111.

[26] R. Supino, MTT assays, in: S. O'Hare, C.K. Atterwill (Eds.), Vitro Toxic. Test. Protoc., Humana Press, Totowa, NJ, 1995, pp. 137–149, https://doi.org/10.1385/0-89603-282-5:137.

[27] M. Ghasemi, T. Turnbull, S. Sebastian, I. Kempson, The MTT assay: utility, limitations, pitfalls, and interpretation in bulk and single-cell analysis, Int. J. Mol. Sci. 22 (2021) 12827, https://doi.org/10.3390/ijms222312827.

[28] F. Awouters, C.J. Niemegeers, F.M. Lenaerts, P.A. Janssen, Delay of castor oil diarrhoea in rats: a new way to evaluate inhibitors of prostaglandin biosynthesis, J. Pharm. Pharmacol. 30 (1978) 41–45, https://doi.org/10.1111/j.2042-7158.1978.tb13150.x.

[29] W. Brand-Williams, M.E. Cuvelier, C. Berset, Use of a free radical method to evaluate antioxidant activity, LWT–Food Sci. Technol. 28 (1995) 25–30, https://doi.org/10.1016/S0023-6438(95)80008-5.

[30] C. Zardecki, S. Dutta, D.S. Goodsell, M. Voigt, S.K. Burley, RCSB protein Data Bank: a resource for chemical, biochemical, and structural explorations of large and small biomolecules, J. Chem. Educ. 93 (2016) 569–575, https://doi.org/10.1021/acs.jchemed.5b00404.

[31] A. Daina, O. Michielin, V. Zoete, SwissADME: a free web tool to evaluate pharmacokinetics, drug-likeness and medicinal chemistry friendliness of small molecules, Sci. Rep. 7 (2017) 1–13, https://doi.org/10.1038/srep42717.

[32] G. Alberghina, A. Arcoria, S. Fisichella, G. Scarlata, Infrared and ultraviolet spectra of some 2-thiophenecarboxamides, Spectrochim. Acta Part A Mol. Spectrosc. 28 (1972) 2063–2068, https://doi.org/10.1016/0584-8539(72)80180-6.

[33] C.K. Lee, J.S. Yu, H.-J. Lee, Determination of aromaticity indices of thiophene and furan by nuclear magnetic resonance spectroscopic analysis of their phenyl esters, J. Heterocycl. Chem. 39 (2002) 1207–1217, https://doi.org/10.1002/jhet.5570390615.

[34] K. Sd, W.-A. H, Physicochemical properties in pharmacokinetic lead optimization, Farm. Soc. Chim. Ital. 1989 (2001) 56, https://doi.org/10.1016/s0014-827x(01)01028-x.

[35] A. Grover, E. Pawar, G.K. Singh, A. Gupta, A. Pareek, R. Desai, I. Purkait, Aceclofenac, a preferential COX-2 inhibitor - appraisal of safety and tolerability, J. Evol. Med. Dent. Sci. (2022) 690–698, https://doi.org/10.14260/jemds.v11i7.148.

[36] M. Rudrapal, W.A. Eltayeb, G. Rakshit, A.A. El-Arabey, J. Khan, S.M. Aldosari, B. Alshehri, M. Abdalla, Dual synergistic inhibition of COX and LOX by potential chemicals from Indian daily spices investigated through detailed computational studies, Sci. Rep. 13 (2023) 8656, https://doi.org/10.1038/s41598-023-35161-0.

[37] A.S. Gilbert, Hydrogen bonding and other physicochemical interactions studied by IR and Raman spectroscopy, in: J.C. Lindon (Ed.), Encycl. Spectrosc. Spectrom, second ed., Academic Press, Oxford, 1999, pp. 957–962, https://doi.org/10.1016/B978-0-12-374413-5.00339-0.

[38] R.C. Wade, P.J. Goodford, The role of hydrogen-bonds in drug binding, Prog. Clin. Biol. Res. 289 (1989) 433–444.

[39] M. Hawash, M.T. Qaoud, N. Jaradat, S. Abdallah, S. Issa, N. Adnan, M. Hoshya, S. Sobuh, Z. Hawash, Anticancer activity of thiophene carboxamide derivatives as CA-4 biomimetics: synthesis, biological potency, 3D spheroid model, and molecular dynamics simulation, Biomimetics 7 (2022) 247, https://doi.org/10.3390/biomimetics7040247.

[40] M. Hawash, N. Jaradat, R. Sabobeh, M. Abualhasan, M.T. Qaoud, New thiazole carboxamide derivatives as COX inhibitors: design, synthesis, anticancer screening, in silico molecular docking, and ADME profile studies, ACS Omega 8 (2023) 29512–29526, https://doi.org/10.1021/acsomega.3c03256.

[41] O.M. Hendawy, H.A.M. Gomaa, S.I. Alzarea, M.S. Alshammari, F.A.M. Mohamed, Y.A. Mostafa, A.H. Abdelazeem, M.H. Abdelrahman, L. Trembleau, B.G. M. Youssif, Novel 1,5-diaryl pyrazole-3-carboxamides as selective COX-2/sEH inhibitors with analgesic, anti-inflammatory, and lower cardiotoxicity effects, Bioorganic Chem 116 (2021) 105302, https://doi.org/10.1016/j.bioorg.2021.105302.

[42] V.Y. Horishny, P.V. Zadorozhnii, I.V. Horishnia, V.S. Matiychuk, Synthesis, anti-inflammatory activity and molecular docking studies of 1,4,5,6-tetrahydropyrimidine-2-carboxamides, Pharm. Sci. 27 (2020) 353–365, https://doi.org/10.34172/PS.2020.100.

[43] E.M. Conner, M.B. Grisham, Inflammation, free radicals, and antioxidants, Nutrition 12 (1996) 274–277, https://doi.org/10.1016/S0899-9007(96)00000-8.

[44] B. Andrade, C. Jara-Gutiérrez, M. Paz-Araos, M.C. Vázquez, P. Díaz, P. Murgas, The relationship between reactive oxygen species and the cGAS/STING signaling pathway in the inflammaging process, Int. J. Mol. Sci. 23 (2022) 15182, https://doi.org/10.3390/ijms232315182.

[45] I.K. Valeeva, A.F. Titarenko, V.N. Khaziakhmetova, L.E. Ziganshina, Anti-inflammatory and anti-oxidant properties: is there a link? Int. J. Risk Saf. Med. 27 (Suppl 1) (2015) S67–S68, https://doi.org/10.3233/JRS-150693.

[46] R. Eglen, Muscarinic receptors and gastrointestinal tract smooth muscle function, Life Sci. 68 (2001) 2573–2578, https://doi.org/10.1016/S0024-3205(01)01054-2.

[47] A.M. Harrington, J.M. Hutson, B.R. Southwell, Cholinergic neurotransmission and muscarinic receptors in the enteric nervous system, Prog. Histochem. Cytochem. 44 (2010) 173–202, https://doi.org/10.1016/j.proghi.2009.10.001.

[48] P. Holzer, Opioid receptors in the gastrointestinal tract, Regul. Pept. 155 (2009) 11–17, https://doi.org/10.1016/j.regpep.2009.03.012.

[49] A. Shahbazian, A. Heinemann, H. Schmidhammer, E. Beubler, U. Holzer-Petsche, P. Holzer, Involvement of μ- and κ-, but not δ-, opioid receptors in the peristaltic motor depression caused by endogenous and exogenous opioids in the Guinea-pig intestine, Br. J. Pharmacol. 135 (2002) 741–750, https://doi.org/10.1038/sj.bjp.0704527.

[50] K. Wesnes, R. Lipton, K. Kolodner, C. Edgar, 513 Darifenacin, an M3 selective receptor antagonist for the treatment of overactive bladder, does not affect cognitive function in elderly volunteers, Eur. Urol. Suppl. 3 (2004) 131, https://doi.org/10.1016/S1569-9056(04)90510-6.

[51] M. Mitsuya, K. Kobayashi, K. Kawakami, A. Satoh, Y. Ogino, T. Kakikawa, N. Ohtake, T. Kimura, H. Hirose, A. Sato, T. Numazawa, T. Hasegawa, K. Noguchi, T. Mase, A potent, long-acting, orally active (2R)-2-[(1R)-3, 3-difluorocyclopentyl]-2-hydroxy-2-phenylacetamide: novel muscarinic M(3) receptor antagonist with high selectivity for M(3) over M(2) receptors, J. Med. Chem. 43 (2000) 5017–5029, https://doi.org/10.1021/jm0003135.

[52] Y. Sagara, M. Mitsuya, M. Uchiyama, Y. Ogino, T. Kimura, N. Ohtake, T. Mase, Discovery of 2-aminothiazole-4-carboxamides, a novel class of muscarinic M(3) selective antagonists, through solution-phase parallel synthesis, Chem. Pharm. Bull. (Tokyo) 53 (2005) 437–440, https://doi.org/10.1248/cpb.53.437.
[53] A.O. El-Abd, S.M. Bayomi, A.K. El-Damasy, B. Mansour, N.I. Abdel-Aziz, M.A. El-Sherbeny, Synthesis and molecular docking study of new thiazole derivatives as potential tubulin polymerization inhibitors, ACS Omega 7 (2022) 33599–33613, https://doi.org/10.1021/acsomega.2c05077.
[54] V. Ghanta, N. Madala, A. Pasula, S.K. Pindiprolu, K. Battula, P. Krishnamurthy, B. Raman, Novel dermacozine-1-carboxamides as promising anticancer agents with tubulin polymerization inhibitory activity, RSC Adv. 9 (2019) 18670–18677, https://doi.org/10.1039/C9RA02416F.
[55] K. Laxmikeshav, P. Sharma, M. Palepu, P. Sharma, A. Mahale, J. George, R. Phanindranath, M.P. Dandekar, O.P. Kulkarni, N. Nagesh, N. Shankaraiah, Benzimidazole based bis-carboxamide derivatives as promising cytotoxic agents: design, synthesis, in silico and tubulin polymerization inhibition, J. Mol. Struct. 1271 (2023) 134078, https://doi.org/10.1016/j.molstruc.2022.134078.
[56] B. Shwetha, M.S. Sudhanva, G.S. Jagadeesha, N.R. Thimmegowda, V.K. Hamse, B.T. Sridhar, K.N. Thimmaiah, C.S. Ananda Kumar, R. Shobith, K.S. Rangappa, Furan-2-carboxamide derivative, a novel microtubule stabilizing agent induces mitotic arrest and potentiates apoptosis in cancer cells, Bioorganic Chem 108 (2021) 104586, https://doi.org/10.1016/j.bioorg.2020.104586.
[57] S. Boichuk, A. Galembikova, K. Syuzov, P. Dunaev, F. Bikinieva, A. Aukhadieva, S. Zykova, N. Igidov, K. Gankova, M. Novikova, P. Kopnin, The design, synthesis, and biological activities of pyrrole-based carboxamides: the novel tubulin inhibitors targeting the colchicine-binding site, Molecules 26 (2021) 5780, https://doi.org/10.3390/molecules26195780.
[58] C. Jadala, M. Sathish, T.S. Reddy, V.G. Reddy, R. Tokala, S.K. Bhargava, N. Shankaraiah, N. Nagesh, A. Kamal, Synthesis and in vitro cytotoxicity evaluation of β-carboline-combretastatin carboxamides as apoptosis inducing agents: DNA intercalation and topoisomerase-II inhibition, Bioorg. Med. Chem. 27 (2019) 3285–3298, https://doi.org/10.1016/j.bmc.2019.06.007.
[59] N.M. Abd El-Fadeal, M.S. Nafie, M.K. El-kherbetawy, A. El-mistekawy, H.M.F. Mohammad, A.M. Elbahaie, A.A. Hashish, S.Y. Alomar, S.Y. Aloyouni, M. El-dosoky, K.M. Morsy, S.A. Zaitone, Antitumor activity of nitazoxanide against colon cancers: molecular docking and experimental studies based on wnt/β-catenin signaling inhibition, Int. J. Mol. Sci. 22 (2021) 5213, https://doi.org/10.3390/ijms22105213.
[60] S.A. Khan, T.K.W. Lee, Investigations of nitazoxanide molecular targets and pathways for the treatment of hepatocellular carcinoma using network pharmacology and molecular docking, Front. Pharmacol. 13 (2022). https://www.frontiersin.org/journals/pharmacology/articles/10.3389/fphar.2022.968148. (Accessed 14 February 2024).
[61] X. Bai, Y. Li, H. Zhang, F. Wang, H. He, J. Yao, L. Liu, S. Li, Role of matrix metalloproteinase-9 in transforming growth factor-β1-induced epithelial–mesenchymal transition in esophageal squamous cell carcinoma, OncoTargets Ther. 10 (2017) 2837–2847, https://doi.org/10.2147/OTT.S134813.
[62] A.G.J. Van Der Zee, E.G.E. De Vries, H. Hollema, S.B. Kaye, R. Brown, W.N. Keith, Molecular analysis of the topoisomerase II α gene and its expression in human ovarian cancer, Ann. Oncol. 5 (1994) 75–81, https://doi.org/10.1093/oxfordjournals.annonc.a058700.
[63] W. Zhang, R. He, S. Chen, L. Zhang, G. Cao, W. Yang, J. Li, The JAM-B/c-src/MMP9 pathway is associated with progression and regulates the invasion of pancreatic cancer, J. Cancer 11 (2020) 3246–3255, https://doi.org/10.7150/jca.40953.
[64] A. Hartley, I. Ahmad, The role of PPARγ in prostate cancer development and progression, Br. J. Cancer 128 (2023) 940–945, https://doi.org/10.1038/s41416-022-02096-8.
[65] A.L. Parker, M. Kavallaris, J.A. McCarroll, Microtubules and their role in cellular stress in cancer, Front. Oncol. 4 (2014) 153, https://doi.org/10.3389/fonc.2014.00153.
[66] J.J. Dannenberg, An Introduction to Hydrogen Bonding By George A. Jeffrey (University of Pittsburgh). Oxford University Press: New York and Oxford. 1997. ix + 303 pp. $60.00. ISBN 0-19-509549-9, J. Am. Chem. Soc. 120 (1998), https://doi.org/10.1021/ja9756331, 5604–5604.
[67] K. Augoff, A. Hryniewicz-Jankowska, R. Tabola, K. Stach, MMP9: A Tough Target for Targeted Therapy for Cancer, Cancers 14 (2022) 1847, https://doi.org/10.3390/cancers14071847.
[68] E. Nuti, A.R. Cantelmo, C. Gallo, A. Bruno, B. Bassani, C. Camodeca, T. Tuccinardi, L. Vera, E. Orlandini, S. Nencetti, E.A. Stura, A. Martinelli, V. Dive, A. Albini, A. Rossello, N-O-Isopropyl Sulfonamido-Based Hydroxamates as Matrix Metalloproteinase Inhibitors: Hit Selection and in Vivo Antiangiogenic Activity, J. Med. Chem. 58 (2015) 7224–7240, https://doi.org/10.1021/acs.jmedchem.5b00367.
[69] S.M. Abou-Seri, A.A.M. Eissa, M.G.M. Behery, F.A. Omar, Synthesis, in vitro anticancer activity and in silico studies of certain isoxazole-based carboxamides, ureates, and hydrazones as potential inhibitors of VEGFR2, Bioorganic Chem 116 (2021) 105334, https://doi.org/10.1016/j.bioorg.2021.105334.
[70] S. Ke, W. Huang, Z. Zhang, Y. Wang, Y. Zhang, Z. Wu, W. Fang, Z. Wan, Y. Gong, J. Yang, K. Wang, L. Shi, Diarylamine-Guided Carboxamide Derivatives: Synthesis, Biological Evaluation, and Potential Mechanism of Action, Front. Chem. 10 (2022) 953523, https://doi.org/10.3389/fchem.2022.953523.
[71] R.A. Mook, J. Wang, X.-R. Ren, M. Chen, I. Spasojevic, L.S. Barak, H.K. Lyerly, W. Chen, Structure-activity studies of Wnt/β-catenin inhibition in the Niclosamide chemotype: Identification of derivatives with improved drug exposure, Bioorg. Med. Chem. 23 (2015) 5829–5838, https://doi.org/10.1016/j.bmc.2015.07.001.
[72] T. Mukhopadhyay, J. Sasaki, R. Ramesh, J.A. Roth, Mebendazole elicits a potent antitumor effect on human cancer cell lines both in vitro and in vivo, Clin. Cancer Res. Off. J. Am. Assoc. Cancer Res. 8 (2002) 2963–2969.
[73] C.A. Lipinski, F. Lombardo, B.W. Dominy, P.J. Feeney, Experimental and computational approaches to estimate solubility and permeability in drug discovery and development settings, Adv. Drug Deliv. Rev. 23 (1997) 3–25, https://doi.org/10.1016/S0169-409X(96)00423-1.
[74] I. Hubatsch, E.G.E. Ragnarsson, P. Artursson, Determination of drug permeability and prediction of drug absorption in Caco-2 monolayers, Nat. Protoc. 2 (2007) 2111–2119, https://doi.org/10.1038/nprot.2007.303.